Structural Principles of Group 14 Icosahedral Hydrides and Elemental Nanostructures of Phosphorus and Arsenic

Antti Karttunen

Department of Chemistry
University of Joensuu
Finland

Joensuu 2007

Antti Karttunen
Department of Chemistry, University of Joensuu
P. O. Box 111, FI-80101 Joensuu, Finland

Supervisor
Prof. Tapani Pakkanen, University of Joensuu

Referees
Prof. Hannu Häkkinen, University of Jyväskylä
Prof. Risto Laitinen, University of Oulu

Opponent
Prof. Pekka Pyykkö, University of Helsinki

To be presented with the permission of the Faculty of Science of the University of Joensuu for public criticism in Auditorium K1, Yliopistokatu 7, Joensuu, on June 14th, 2007, at 12 o'clock noon.

ISSN 1456-3975
ISBN 978-952-458-995-6 (PDF)

Joensuun yliopistopaino
Joensuu 2007

ABSTRACT

Knowledge of the exact molecular structures of nanostructures greatly facilitates their further modification and functionalization. For example, carbon nanostructures such as the fullerenes and carbon nanotubes have been studied extensively because their structural principles are well-known. Despite the important role of the fullerenes in nanochemistry, their fully hydrogenated counterparts, fulleranes, are not well understood. Synthesis of the fulleranes would result in novel hydrocarbon cages, but synthetic attempts focusing on the preparation of $C_{60}H_{60}$ fullerane from the C_{60} fullerene have been unsuccessful so far.

In this work, a novel structural motif of "in–out" isomerism was applied to derive the structures of fully hydrogenated icosahedral fulleranes larger than $C_{60}H_{60}$. In the in–out isomeric cage structures the structural strain is reduced by placing a portion of the hydrogens inside the cage. Partial endo-hydrogenation of icosahedral C_{80} and C_{180} fullerenes resulted in I_h-symmetric $C_{80}H_{80}$ and $C_{180}H_{180}$ fulleranes, which are remarkably stable in comparison with previously studied fulleranes. The high thermodynamical stability of the structures was predicted on the basis of quantum chemical B3LYP and MP2 calculations. Controlled synthesis of the predicted fulleranes would produce hydrocarbon cage structures with promising applications, and their further functionalization could result in a whole new branch of hydrocarbon nanochemistry. The vibrational spectra of the fulleranes suggest their existence in the interstellar medium.

Applying the structural motif of partial endo-hydrogenation to the hydrides of heavier group 14 elements resulted in stable families of I_h-symmetric polysilane, polygermane, and polystannane nanostructures. Calculations on systems up to $Si_{540}H_{540}$, $Ge_{500}H_{500}$, and $Sn_{500}H_{500}$ showed the structures to become increasingly stable as the size of the cage increases. The icosahedral $(SiH)_n$, $(GeH)_n$, and $(SnH)_n$ structures are composed of puckered sheets resembling monolayers of the experimentally known layered polysilyne and polygermyne. The structures, stabilities, and electronic properties of the cages converge towards the experimentally known reference systems. If synthesized in a controlled manner, the polysilane, polygermane, and polystannane nanostructures and their mixtures, with their interesting electronic properties, might find use in optoelectronic applications.

Further extension of the in–out structural motif to phosphorus and arsenic cages, where the hydrogens are replaced by lone electron pairs, produced icosahedral P_n and As_n allotropes, structurally related to black phosphorus and gray arsenic. Another structural motif, based on the building principles of the red allotrope of phosphorus, resulted in ring-shaped chains. Calculations performed on icosahedral cages up to 720 atoms and ring-shaped chains up to 360 atoms showed clear energy trends and distinct differences in the two elements. Phosphorus favors ring-shaped chains over icosahedral cages, while arsenic favors large cages over the rings. Comparisons to the experimentally known allotropic forms indicate that the elemental nanostructures are thermodynamically stable, suggesting their experimental synthesis to be viable.

LIST OF ORIGINAL PUBLICATIONS

This dissertation is a summary of publications I-IV and submitted manuscript V.

I Linnolahti, M.; Karttunen, A.J.; Pakkanen, T.A., Remarkably stable icosahedral fulleranes: $C_{80}H_{80}$and $C_{180}H_{180}$, *ChemPhysChem*, **2006**, *7*, 1661–1663.

II Karttunen, A. J.; Linnolahti, M.; Pakkanen, T. A., Icosahedral polysilane nanostructures, *J. Phys. Chem. C*, **2007**, *111*, 2545–2547.

III Karttunen, A. J.; Linnolahti, M.; Pakkanen, T. A., Icosahedral and ring-shaped allotropes of phosphorus, *Chem. Eur. J.*, **2007**, in press, DOI: 10.1002/chem.200601572.

IV Karttunen, A. J.; Linnolahti, M.; Pakkanen, T. A., Icosahedral polygermane and polystannane nanostructures, *J. Phys. Chem. C*, **2007**, *111*, 6318–6320.

V Karttunen, A. J.; Linnolahti, M.; Pakkanen, T. A., Icosahedral and ring-shaped allotropes of arsenic, submitted for publication.

CONTENTS

ABBREVIATIONS

B3LYP	Becke's three-parameter hybrid density functional with the correlation functional of Lee, Yang, and Parr.
DFT	Density functional theory
ECP	Effective Core Potential
HOMO	Highest occupied molecular orbital
IR	Infrared
LUMO	Lowest unoccupied molecular orbital
MP2	Second-order Møller-Plesset perturbation theory
RI	Resolution-of-the-identity
SVP	Karlsruhe split-valence basis set with polarization functions
TZVP	Karlsruhe triple zeta valence basis set with polarization functions
ZPE	Zero-point energy

1. INTRODUCTION

1.1. PREDICTION OF MOLECULAR STRUCTURES WITH QUANTUM CHEMICAL METHODS

The discovery of nanostructures such as the fullerenes and carbon nanotubes has revealed unexpected structural principles, suggesting that further new species could be predicted by the systematic application of novel structural motifs. The structures of fullerene hydrides and their heavier group 14 counterparts are less well known than those of fullerenes, making them a suitable target for systematic study. Given the diverse allotropy of phosphorus and arsenic, the analogous structures these elements are another promising source of previously unknown nanostructures. Modern quantum chemical methods are a powerful tool for the evaluation of structures, stabilities, and properties of chemical compounds, making it possible to predict the existence of molecular structures not yet synthesized.

1.2. FULLERANES

Fulleranes are the fully hydrogenated counterparts of fullerenes. Thus, full hydrogenation of buckminsterfullerene, C_{60},[1] would lead to a $C_{60}H_{60}$ fullerane (Figure 1). The fulleranes have been investigated extensively ever since the fullerenes became available in gram quantities in 1990,[2] the most efforts to produce fulleranes having been focused on the hydrogenation of C_{60}.[3] However, despite the attempts to produce perhydrogenated fulleranes, only partially hydrogenated structures have been synthesized so far.[3] The fulleranes are an attractive synthetic target because of several promising applications, one being the storage of hydrogen.[3] Furthermore, their successful functionalization could open up a whole new branch of chemistry. In addition to the various interesting chemical applications, the fulleranes might also play a role in astrochemistry. Unidentified astronomical emission features occurring at 2800–3100 cm^{-1} are interpreted to originate from hydrocarbons,[4] and the fulleranes have been suggested as one possible source of the emission features.[5]

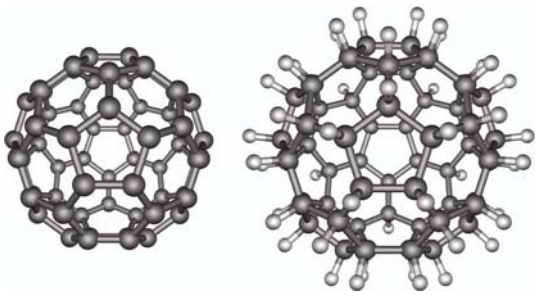

Figure 1. C_{60} fullerene (left) and $C_{60}H_{60}$ fullerane (right).

1.3. POLYSILANES, POLYGERMANES, AND POLYSTANNANES

Inorganic polymers often possess properties not found in their organic counterparts. Polysilanes,[6] polygermanes,[7] and polystannanes,[7] the catenates of silicon, germanium, and tin, possess optical and electronic properties not found in the analogous carbon polymers. The optical properties are associated with the delocalization of the σ-electrons in the polymer backbone,[6,7] an effect not present in the corresponding sp^3-hybridized structures of carbon.

Numerous polysilane, polygermane, and polystannane structures have been prepared. Small polyhedral cages such as tetrahedranes,[8,9] prismanes,[10] and cubanes[11] are strained, and their syntheses require the presence of bulky substituents. In general, the strain of the group 14 polyhedral cages has been shown to decrease in the order C > Si > Ge > Sn, the larger polyhedral cages of Si, Ge, and Sn being noticeably less strained than their carbon analogues.[12,13] Many linear and branched polysilane, polygermane, and polystannane chains have been synthesized to date.[6,7,14] Polysilynes, $(SiR)_n$, and polygermynes, $(GeR)_n$, can be prepared as random-network polymers[15,16] or ordered three-dimensional layer structures.[17,18] The structurally characterized forms of polysilyne and polygermyne, the layered polysilyne, $(SiH)_n$,[17] (Figure 2) and layered polygermyne, $(GeH)_n$,[18] have closely similar structures and electronic properties.[19,20]

Modifying the structure or chemical composition of the polymer backbone influences the optical properties of the group 14 polymers. The systematic engineering of optical and electronic properties such as efficient photoluminescence might turn out to be useful in optoelectronics, for instance.[21]

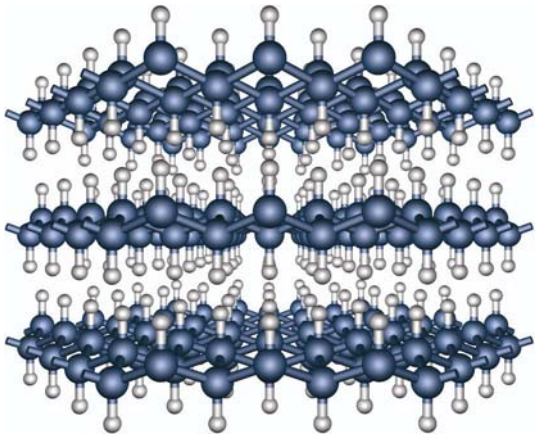

Figure 2. Layered polysilyne $(SiH)_n$. The monolayers of the structure are structurally equivalent to those of layered polygermyne, $(GeH)_n$, but the stacking of the layers is less complex.

1.4. ALLOTROPY OF PHOSPHORUS AND ARSENIC

Elements with diverse allotropic modifications are promising sources for elemental nanostructures. Group 15 elements phosphorus and arsenic both exist in several allotropic forms. The allotropes of phosphorus are usually divided into three main classes, denoted as white, red, and black phosphorus on the basis of their macroscopic appearance.[22] White phosphorus is composed of tetrahedral P_4 molecules (Figure 3),[23] while the red and black allotropes adopt several different structures. At atmospheric pressure, black phosphorus has an orthorhombic crystal structure,[24] which can be converted to rhombohedral or cubic form by increasing the pressure (Figure 3).[25] The red phosphorus usually forms amorphous polymeric networks, making the determination of its structure difficult. So far, the only structurally characterized forms of the red phosphorus are violet[26] and fibrous red[27] phosphorus, both composed of layered pentagonal tubes (Figure 3). Additionally, various red phosphorus chains can be obtained embedded in copper–halide matrices,[28] two of these chains having been isolated as phosphorus nanorods.[29]

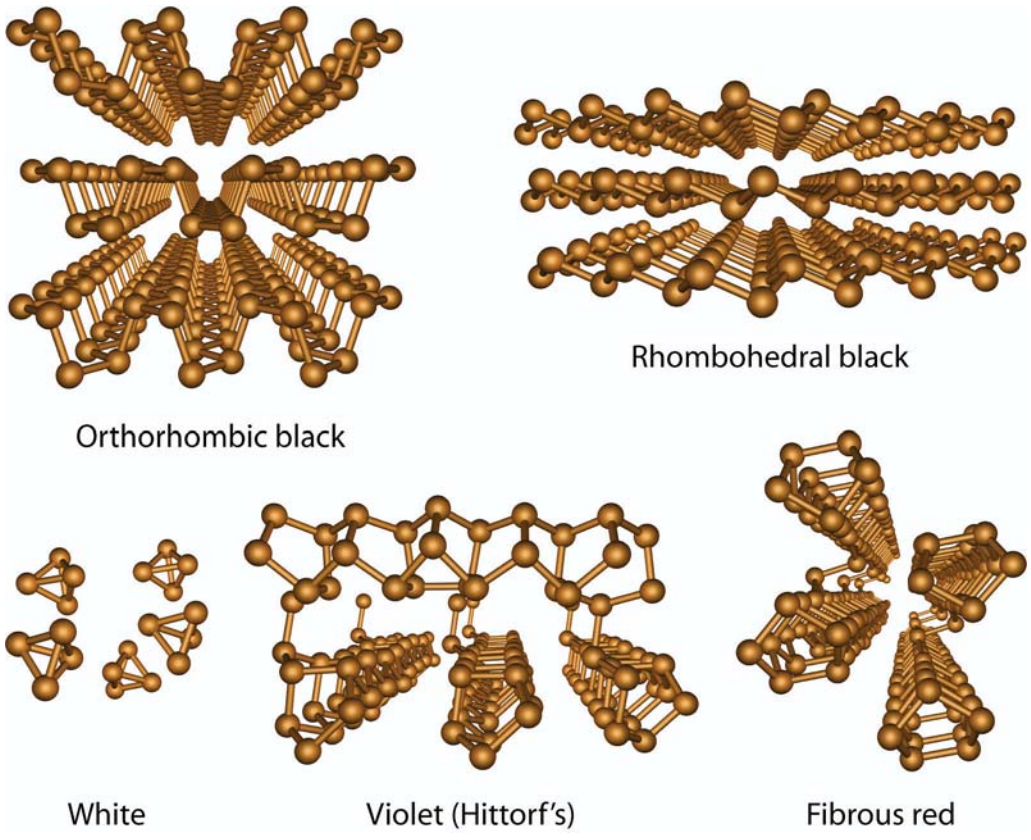

Figure 3. Various allotropes of phosphorus. For clarity, only a single parallel tube of violet phosphorus is shown.

Arsenic has several allotropic forms analogous to those of phosphorus.[30] The most stable allotrope at room temperature, the rhombohedral gray arsenic,[31] is structurally equivalent to the rhombohedral black phosphorus. Arsenic also has an orthorhombic polymorph analogous to orthorhombic black phosphorus.[32] Yellow arsenic is composed of As_4 tetrahedra, being the arsenic counterpart of the white phosphorus.[30] Arsenic structures corresponding to the red allotrope of phosphorus have so far been obtained only as mixtures of phosphorus and arsenic. P–As chains with arsenic content up to 55% have been prepared by copper–halide matrix embedding techniques.[33] The mixed P–As chains can be further isolated from the matrix, resulting in semiconducting P–As polymers.[34] Various amounts of arsenic can also be incorporated in the structures of violet,[35] white,[36] and black phosphorus.[37]

1.5. AIM OF THE STUDY

The starting point for the study was the discovery of the novel structural motif of "in–out" isomerism, first realized for icosahedral fulleranes. The aim of the work was to systematically apply the novel building principles to a series of inorganic compounds of groups 14 and 15, and to study their thermodynamical stabilities and electronic properties by quantum chemical methods.

The structures of the heavier group 14 icosahedral hydrides are derived from the structures of the icosahedral fulleranes. However, the stabilities and properties of the resulting polysilane, polygermane, and polystannane structures may be very different from those of the fulleranes.

Group 15 elements phosphorus and arsenic are considered to investigate the applicability of the in–out isomerism to cases where the hydrogens are replaced by lone electron pairs. Additionally, it was thought that further application of the structural principles of the different allotropes of phosphorus and arsenic might reveal previously unknown elemental nanostructures.

To assess the synthetic viability of the predicted structures, their thermodynamical stabilities are compared with those of experimentally known compounds, where feasible. Knowledge of the relative thermodynamical stabilities of the compounds allows a discussion of possible approaches to their experimental preparation.

2. COMPUTATIONAL METHODS

This study consists of quantum chemical calculations on molecular structures together with periodic calculations on systems extending in one, two, or three dimensions. The molecular structures were fully optimized within their respective point group symmetries by using the B3LYP hybrid density functional,[38] which has been shown to be a well-performing functional for compounds consisting of main group elements.[39] The quantum chemical program package TURBOMOLE was used in the molecular calculations.[40] The one- and two-dimensional periodic structures and the structure of the layered polysilane[II] were fully optimized with the B3LYP method, while the experimental cell parameters were retained for the crystal structures of violet and fibrous red phosphorus.[III] The periodic calculations reported in papers I and V were carried out with the Gaussian 03 software,[41] and the calculations reported in papers II–IV with the CRYSTAL program.[42]

The basis sets used in B3LYP calculations had to be carefully chosen to enable comparisons between molecular and periodic structures. In periodic calculations, where the atoms are closely packed throughout the space, very large basis sets designed for molecular calculations are often excessive.[43] Using moderate-sized basis sets also allows studies on nanostructures with hundreds of atoms. Generally, split-valence quality basis sets with polarization functions were used for all atoms. The studies on fulleranes[I] and polysilanes[II] applied modified 6-21G* basis sets for carbon[44] and silicon,[45] while the standard 6-31G** basis set was used for hydrogen.[46] The allotropes of phosphorus were investigated using a 85-21G* basis set[47] optimized for systems containing only phosphorus.[III] In the case of polygermanes,[IV] polystannanes,[IV] and allotropes of arsenic,[V] it was possible to use the Karlsruhe molecular SVP basis sets for all atoms.[48] The basis set applied for tin made use of a 28-electron effective core potential[49] (ECP) to account for relativistic effects, which are known to be important for heavier atoms.[50]

In addition to the B3LYP calculations, *ab initio* MP2 calculations were performed on various molecular structures using the resolution-of-the-identity (RI) approximation as implemented in TURBOMOLE.[51] MP2 is computationally more demanding than B3LYP, but it takes dispersion forces into account.[52] The structures of the fulleranes were fully optimized by the MP2 method,[I] while the MP2 calculations on the other compounds were performed at the B3LYP optimized geometries.[II–V] An all-electron triple zeta valence basis set with polarization functions (TZVP)[53] and the corresponding RI auxiliary basis set[54] were used for all atoms except Sn. Tin was described using a 28-electron ECP[49] and a TZVP basis set[55] together with an RI auxiliary basis set.[56]

To confirm the vibrational stability of the structures and to obtain Gibbs free energies, B3LYP vibrational frequency calculations were performed on the molecular structures, where feasible.[57] A zero-point vibrational energy scaling factor of 0.9806 was adopted for the calculation of Gibbs free energies.[58] The infrared frequency wavenumbers presented for fulleranes[I] were obtained using a harmonic frequency scaling factor of 0.9614.[58]

3. ICOSAHEDRAL FULLERANES[I]

3.1. STRUCTURES AND STABILITIES

The only experimentally known icosahedral fullerane is the $C_{20}H_{20}$ dodecahedrane (Figure 4), synthesized in 1982 by Paquette et al.[59] Dodecahedrane is composed of 12 five-membered rings, resulting in bond angles of 108°, nearly optimal for sp^3 hybridization. As a consequence, dodecahedrane has the lowest strain energy of all polyhedral $(CH)_n$ cages.[60] The next icosahedral fullerane in size is the perhydrogenated counterpart of C_{60} fullerene, the long sought[3] $C_{60}H_{60}$ (Figure 4). However, the 20 sp^2-hybridized six-membered rings present in C_{60} have bond angles of 120°, resulting in a strained structure in sp^3-hybridized $C_{60}H_{60}$. It has been suggested, that the structural strain in $C_{60}H_{60}$ could be decreased by partial endo-hydrogenation.[61,62] Placing hydrogens inside the cage results in puckering of the six-membered rings, allowing them to adopt more optimal bond angles for sp^3 hybridization. However, the puckering of the six-membered rings gives rise to simultaneous puckering of the five-membered rings, breaking their optimal planar arrangement. Thus, even the application of "in–out" isomerism leaves the $C_{60}H_{60}$ much more strained than the experimentally known dodecahedrane.

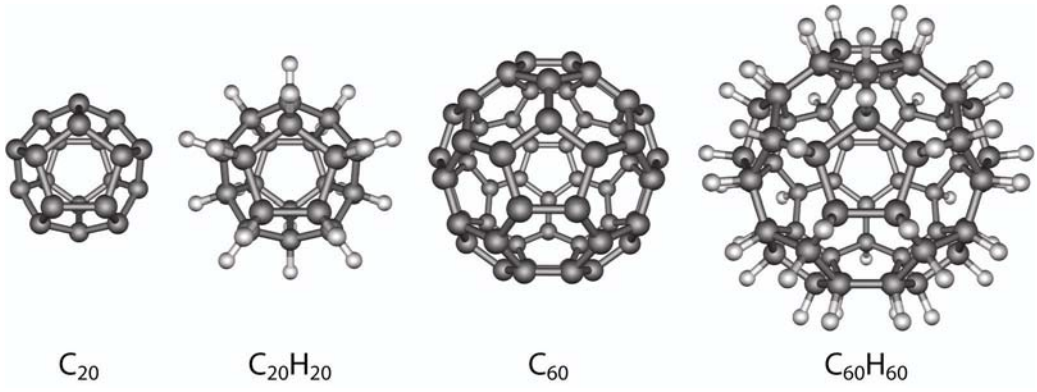

Figure 4. I_h-symmetric C_{20} and C_{60} fullerenes together with their perhydrogenated fullerane counterparts.

Larger I_h-symmetric fullerenes have not been studied as extensively as the buckminsterfullerene, but their larger size enables structural modifications not feasible for C_{60}. In the next I_h-symmetric fullerene C_{80}, the 12 pentagons are linked by 20 interconnecting carbon atoms, each located between a set of three pentagons (Figure 5). Hydrogenation of the interconnecting carbons inside and the other 60 carbons outside results in an I_h-symmetric $C_{80}H_{80}$ fullerane (Figure 5). In the "in–out" isomeric $C_{80}H_{80}$ the pentagons can retain their optimal planar arrangement, while the interconnecting atoms point toward the interior of the cage, puckering the hexagons

into the shape of the boat conformer of cyclohexane. This structural motif allows all carbon atoms to adopt nearly optimal bond angles for sp^3 hybridization, resulting in a remarkably stable species (Table 1). The relative total energy of the in–out isomeric $C_{80}H_{80}$ is lower than that of the experimentally known dodecahedrane, previously shown to be the least strained $(CH)_n$ cage for values of n up to 24.[13,63] At the MP2 level of theory, $C_{80}H_{80}$ is also more stable than $C_{20}H_{20}$ in terms of Gibbs free energy (Table 1).

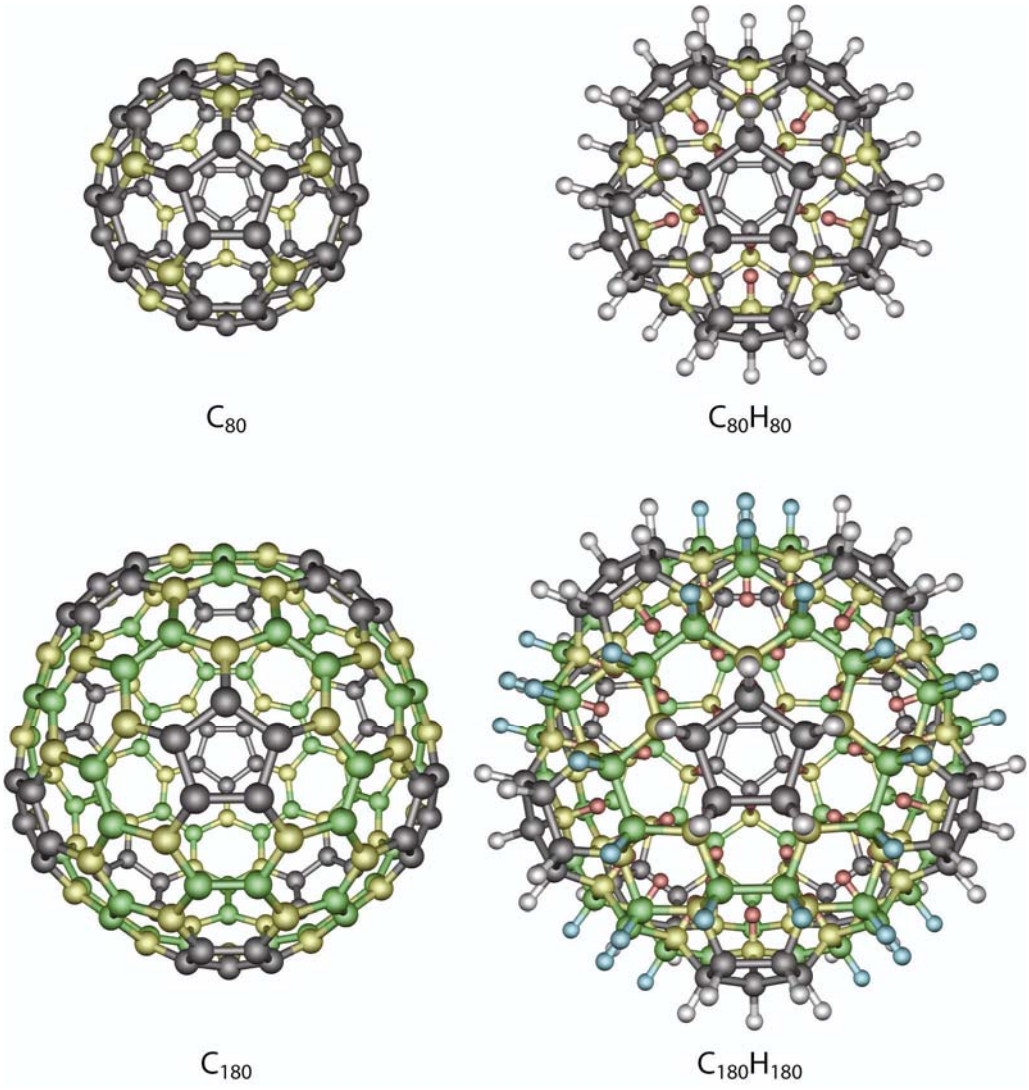

Figure 5. I_h-symmetric C_{80} and C_{180} fullerenes together with their perhydrogenated fullerane counterparts. The colors denote equivalent atoms. Gray: C in pentagon; white: H connected to pentagon; yellow: C of six-membered ring pointing toward the cage center; red: H pointing inward; green: C of six-membered ring pointing outward; blue: H pointing outward from six-membered ring.

The in–out structural motif can also be applied for the next I_h-symmetric fullerene in size, C_{180}, where each of the 20 carbons interconnecting the pentagons is replaced by a hexagon (Figure 5). Alternating in–out hydrogenation of the hexagons together with exterior hydrogenation of the planar pentagons leads to an I_h-symmetric, in–out isomeric $C_{180}H_{180}$ fullerane (Figure 5). In total, 60 hydrogen atoms are located inside the cage. The hexagons interconnecting the sets of three pentagons adopt the chair conformation of cyclohexane, while the hexagons formed between each pair of pentagons are boat-shaped. The in–out isomeric $C_{180}H_{180}$ cage has even lower relative total energy than the smaller $C_{80}H_{80}$ (Table 1), demonstrating the favorable effect of the puckering of the cage.

Further enlargement of the I_h-symmetric fulleranes would increase the relative proportion of the puckered hexagons. The hexagons adopting the chair conformation of cyclohexane form the 20 faces of an icosahedron, and the structures of very large in–out isomeric fulleranes can be described as cages sewed together from 20 hydrogenated diamond (111) slabs. Each slab is composed of puckered hexagons in the shape of the chair conformer of cyclohexane (Figure 6).

Because the infinite hydrogenated diamond (111) slab has no curvature, it can be considered as a strain-free reference system for the fullerane cages. Thus, the strain energy of each fullerane cage is equal to the energy difference between the cage and the hydrogenated diamond (111) slab (Table 1). The B3LYP-calculated strain energies of $C_{20}H_{20}$, $C_{80}H_{80}$, and $C_{180}H_{180}$ are 14.8, 13.6, and 9.9 kJ/mol per CH unit, respectively, their structures and stabilities approaching those of the hydrogenated diamond (111) slab. For comparison, the strain energy of $C_{60}H_{60}$ is 43.6 kJ/mol per CH unit, showing that this structure is highly strained in comparison with the other studied fulleranes.

Table 1. Relative total energies, Gibbs free energies (T = 298.15K),[a] and diameters of the four smallest I_h-symmetric perhydrogenated fulleranes together with the hydrogenated diamond (111) slab, $C_\infty H_\infty$.

	ΔE_{B3LYP}	ΔG_{B3LYP}	ΔE_{MP2}	ΔG_{MP2}[b]	Diameter (nm)[c]
$C_{20}H_{20}$	0.0	0.0	0.0	0.0	0.66
$C_{60}H_{60}$	28.8	32.1	32.0	35.2	0.99
$C_{80}H_{80}$	–1.2	1.8	–4.9	–2.0	1.09
$C_{180}H_{180}$	–4.9	–1.5	–8.4[d]	–5.0[d]	1.55
$C_\infty H_\infty$	–14.8				

[a] The energies in kJ/mol per CH unit are given relative to $C_{20}H_{20}$.
[b] Gibbs corrections for total energy obtained from B3LYP calculations.
[c] B3LYP value. MP2 diameters are within 0.01 nm of the B3LYP values.
[d] Previously unpublished result.

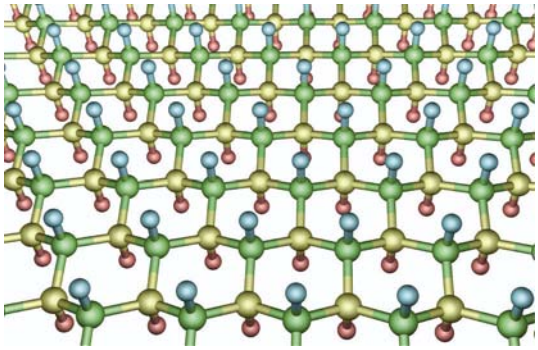

Figure 6. Hydrogenated diamond (111) slab. For interpretation of the colors, see Figure 5.

Several synthetic techniques might be feasible for the preparation of the fulleranes, the methods used to partially hydrogenate C_{60} already being well established.[3] Partially hydrogenated fullerenes and carbon nanotubes have also been produced by reactions with hydrogen plasma.[64] Hydrocarbon nano-onions, the possible multiwalled analogues of the icosahedral fulleranes, may have been produced via sonochemical reactions.[65] The molecular structures of the synthesized structures have not yet been characterized. Fulleranes may also exist in mixtures of large hydrocarbons such as bitumen.

Controlled synthesis of the predicted icosahedral fulleranes with subsequent functionalization could open up a new branch of chemistry. Numerous derivatives of the fulleranes could be designed and produced using the synthetic approaches developed for hydrocarbons over the years. Fluorinated fulleranes such as $C_{60}F_{60}$ have been predicted to be superior lubricants.[66] While a fluorinated fullerane based on C_{60} might be difficult to produce due to structural strain, a spherical I_h-symmetric $C_{80}H_{20}F_{60}$ based on in–out isomeric $C_{80}H_{80}$ could turn out to be a feasible synthetic target.

3.2. SPECTRAL FEATURES

The fulleranes have been suggested as a possible source of unidentified astronomical infrared emission features measured from various interstellar objects.[5] The unidentified features occur at the typical wavelengths of sp^3-hybridized C–H stretching vibrations, showing a plateau of emissions from 2800 to 3100 cm^{-1} with peaks at 2800, 2850, 2890, 2940, and 3040 cm^{-1}.[4]

The astrochemical role of the fulleranes can be studied by investigating their calculated IR spectra at the typical C–H stretching wavelengths. The B3LYP vibrational spectra of the four smallest I_h-symmetric fulleranes at 2700–3100 cm^{-1} are shown in Figure 7. All CH units in $C_{20}H_{20}$ and in $C_{60}H_{60}$ are equivalent, resulting in only one C–H stretching vibration per cage, at 2920 and 2950 cm^{-1}, respectively. The value of 2920 cm^{-1} for $C_{20}H_{20}$ is comparable to the experimental value of 2945 cm^{-1}.[59]

Three different C–H stretching vibrations are seen in the IR spectrum of $C_{80}H_{80}$: the C–H bonds outside the cage vibrate at 2870 and 2890 cm^{-1}, while the C–H stretching vibration inside the cage occurs at 2960 cm^{-1}. Corresponding vibrations, shifted to lower wavelengths, are seen in the spectrum of $C_{180}H_{180}$, together with a fourth vibration at 2820 cm^{-1} due to C–H stretching outwards from the hexagons. The C–H stretching vibrations of $C_{180}H_{180}$ at 2820, 2860, 2890, and 2920 cm^{-1} resemble the experimentally observed astronomical IR emissions occurring at 2800, 2850, 2890, and 2940 cm^{-1}. The total number of IR-active C–H stretching vibrations in $C_{180}H_{180}$ is six, the vibrations at 2850 and 2880 cm^{-1} being shoulders of the main vibrations at 2860 and 2890 cm^{-1}, respectively.

The fifth unidentified astronomical emission feature, at 3040 cm^{-1}, is located at the typical wavenumber of sp^2 aromatic C–H stretching. Therefore it is likely to originate from polycyclic aromatic hydrocarbons[67] or aromatic fragments of C_{60} liberated during extensive exposure to atomic hydrogen.[68]

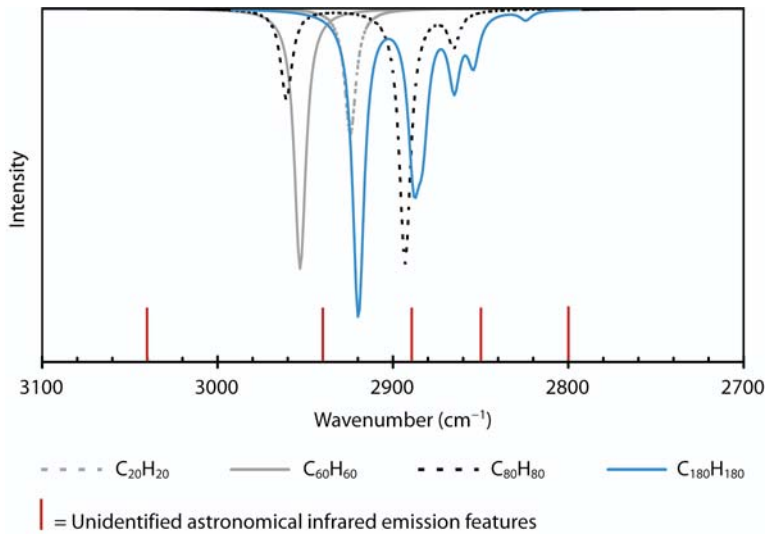

Figure 7. Calculated infrared spectra at 2700–3100 cm^{-1} for the four smallest I_h-symmetric perhydrogenated fulleranes, together with unidentified astronomical infrared emission features.

4. ICOSAHEDRAL POLYSILANES, POLYGERMANES, AND POLYSTANNANES[II, IV]

4.1. STRUCTURES AND STABILITIES

The heavier elements of group 14 are known to form polyhedral structures similar to carbon.[9] However, the experimentally known polyhedral cages of silicon, germanium, and tin are limited to the smaller polyhedra,[8,10,11] dodecahedral cages analogous to $C_{20}H_{20}$ not having been synthesized so far. Theoretical studies have shown the perhydrogenated dodecahedral $Si_{20}H_{20}$, $Ge_{20}H_{20}$, and $Sn_{20}H_{20}$ cages to be less strained than their carbon analogues,[13] and $Si_{20}H_{20}$ has been predicted to be a stable molecule.[69] The I_h-symmetric $Si_{60}H_{60}$ is also considerably less strained than its carbon counterpart $C_{60}H_{60}$, but it is still strained in comparison with $Si_{20}H_{20}$.[9] The cage structures of the heavier elements of group 14 larger than the 60-membered icosahedral cage have not been studied extensively. As in the case of carbon, the enlargement of the cages enables novel structural modifications that have a noticeable stabilizing effect on the fully hydrogenated polyhedral compounds of silicon, germanium, and tin.

The in–out structural motif derived for the icosahedral fulleranes[I] can be applied to the heavier elements of group 14 in a straightforward way. The I_h-symmetric $Si_{80}H_{80}$ polysilane cage adopts a similar puckered structure analogous to that of the in–out isomeric $C_{80}H_{80}$ fullerane (Figure 8). The 12 pentagons retain the planar arrangement optimal for tetrahedral coordination, while the 20 atoms interconnecting each set of three pentagons point toward the cage center. The pentagons are exo-hydrogenated and the interconnecting atoms endo-hydrogenated. The corresponding icosahedral $Ge_{80}H_{80}$ and $Sn_{80}H_{80}$ structures are derived analogously to the $Si_{80}H_{80}$ structure.

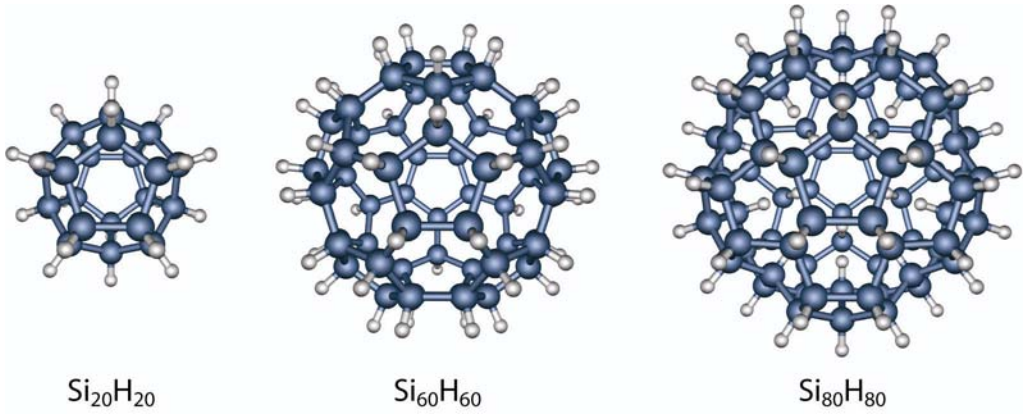

Figure 8. Three smallest I_h-symmetric polysilane cages.

Applying the in–out isomerism to larger I_h-symmetric polysilane, polygermane, and polystannane cages results in two series of I_h-symmetric $(SiH)_n$, $(GeH)_n$, and $(SnH)_n$ structures: (1) n = 20, 80, 180, 320, 500, …, $20m^2$ and (2) n = 60, 240, 540, 960, 1500, …, $60m^2$ (m = 1, 2, 3, …). The series $20m^2$ (Figure 9) is continuation of the dodecahedral $M_{20}H_{20}$ cage (M = Si, Ge, Sn), while the first member of the series $60m^2$ is the $M_{60}H_{60}$ cage with ring topology similar to C_{60} (Figure 10). The difference between the two series is the presence of 20 planar, exo-hydrogenated hexagons in the series $60m^2$. The appearance of the cages is closely similar for all three elements, the polysilanes and polygermanes being nearly equal in size, too.

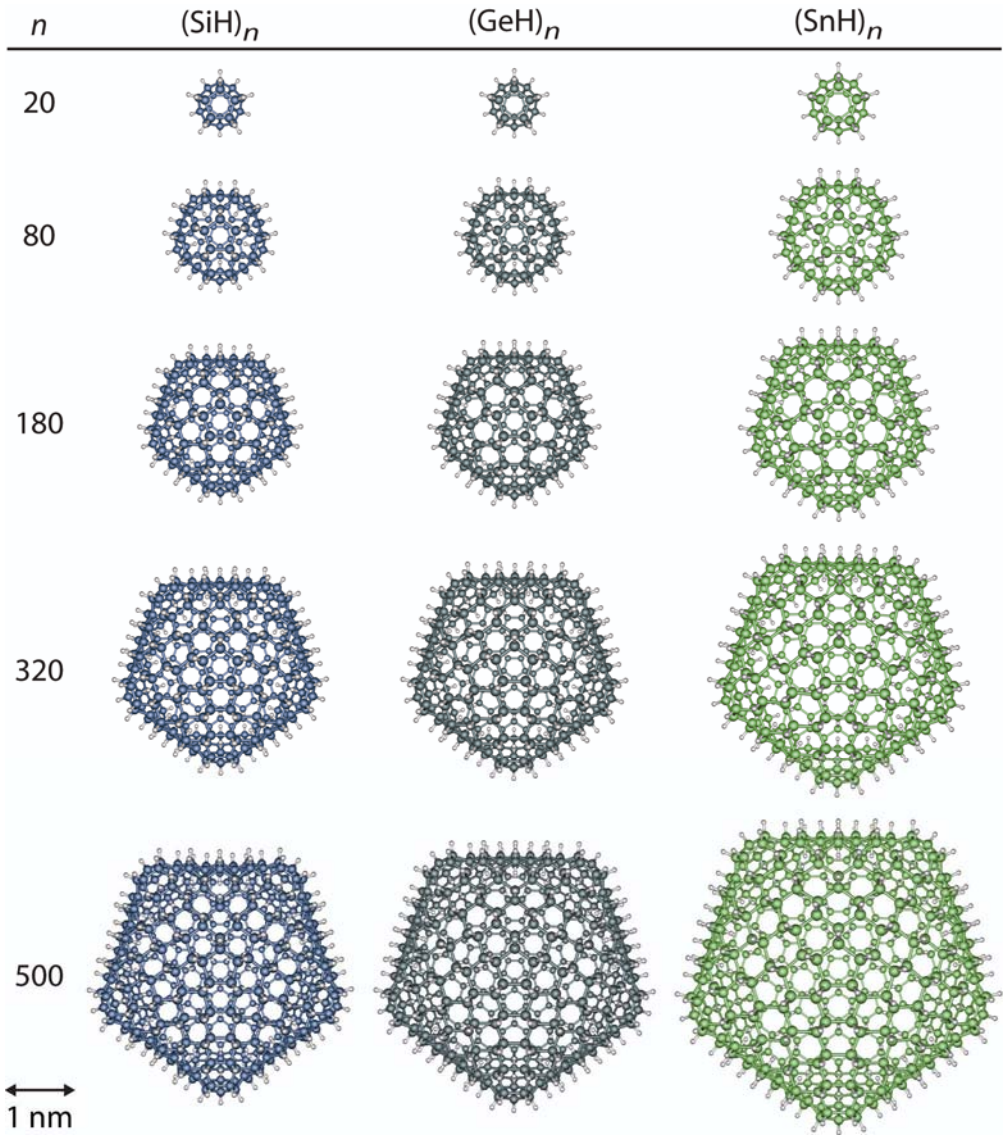

Figure 9. I_h-symmetric polysilane, polygermane, and polystannane cages belonging to the n = $20m^2$ series of structures, with m = 1–5.

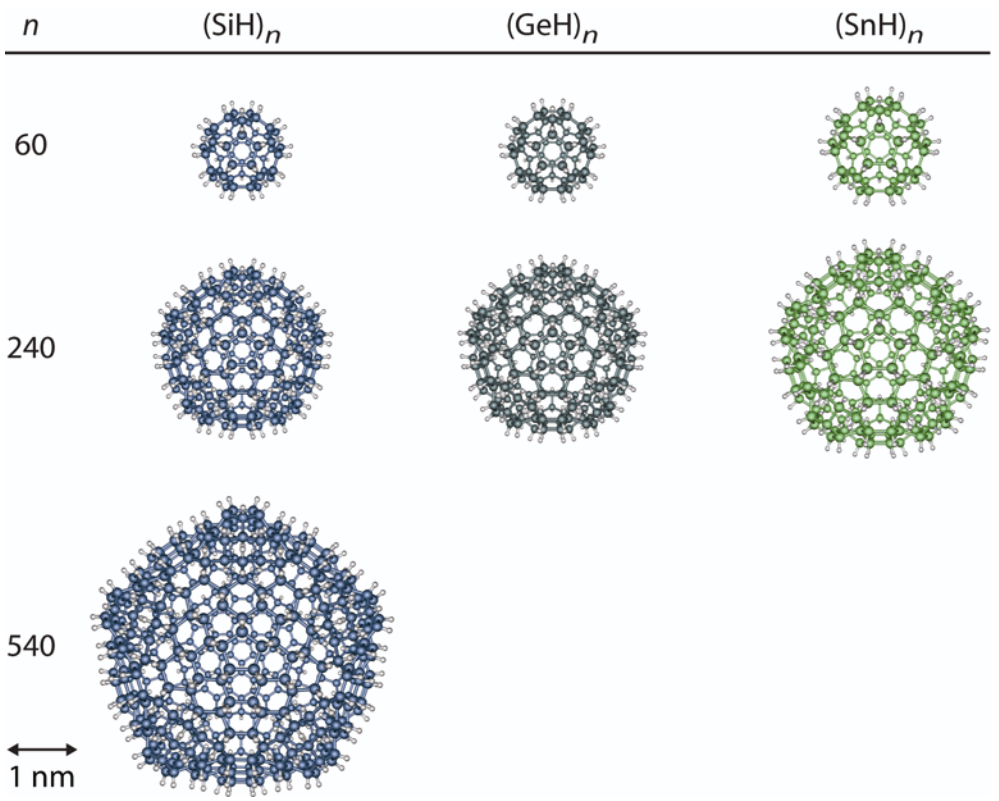

Figure 10. I_h-symmetric polysilane, polygermane, and polystannane cages belonging to the $n = 60m^2$ series of structures, with m = 1–3 for Si and m = 1–2 for Ge and Sn.

The I_h-symmetric $(SiH)_n$, $(GeH)_n$, and $(SnH)_n$ cages become increasingly stable as a function of the size of the cage (Tables 2–4). Series $60m^2$ is less stable than series $20m^2$ due to the structural strain resulting from the presence of 20 exo-hydrogenated planar hexagons. For all three elements, the larger members of the $20m^2$ series are more stable than the dodecahedral $M_{20}H_{20}$ cage. The larger members of the $60m^2$ series also become more stable than $M_{20}H_{20}$, only the $M_{60}H_{60}$ cage being less stable than the dodecahedral $M_{20}H_{20}$.

The ring topologies of the icosahedral $n = 20m^2$ and $n = 60m^2$ cages are analogous to those of the icosahedral $(h,0)$ and (h,k), $h=k$ fullerenes, respectively.[70] The faceted icosahedral shape of the $20m^2$ structures becomes evident as the sizes of the cages increase (Figure 9). The 20 facets of the icosahedra are composed of puckered, in–out isomeric hexagons. Analogously to the icosahedral fulleranes,[I] the structures of the heavier group 14 cages can be considered as 20 monolayer sheets of $(SiH)_n$, $(GeH)_n$, or $(SnH)_n$ sewed into a cage (Figure 11). The $60m^2$ series also adopts a faceted shape, but the total number of facets is 60 because the planar hexagons divide each of the 20 facets into three additional facets.

Table 2. Relative total energies and Gibbs free energies (T = 298.15K),[a] HOMO–LUMO gaps, and diameters of I_h-symmetric polysilanes together with the layered polysilane.

	ΔE_{B3LYP}	ΔG_{B3LYP}	ΔE_{MP2}	ΔG_{MP2}[b]	Gap_{B3LYP} (eV)	Diameter (nm)
Series 20m^2						
$Si_{20}H_{20}$	0.0	0.0	0.0	0.0	5.10	0.96
$Si_{80}H_{80}$	–4.7	–2.4	–7.0	–4.7	4.20	1.63
$Si_{180}H_{180}$	–6.1	–3.5	–8.6	–5.9	4.15	2.34
$Si_{320}H_{320}$	–6.9				3.95	3.06
$Si_{500}H_{500}$	–7.4				3.88	3.77
Series 60m^2						
$Si_{60}H_{60}$	5.4	7.6	6.8	8.9	5.05	1.47
$Si_{240}H_{240}$	–2.4				4.13	2.63
$Si_{540}H_{540}$	–4.8				4.01	3.89
Layered polysilyne	–8.4				3.37	

[a] The energies in kJ/mol per SiH unit are given relative to $Si_{20}H_{20}$.
[b] Gibbs corrections for total energy obtained from B3LYP calculations.

Table 3. Relative total energies and Gibbs free energies (T = 298.15K),[a] HOMO–LUMO gaps, and diameters of I_h-symmetric polygermanes together with the infinite GeH sheet.

	ΔE_{B3LYP}	ΔG_{B3LYP}	ΔE_{MP2}	ΔG_{MP2}[b]	Gap_{B3LYP} (eV)	Diameter (nm)
Series 20m^2						
$Ge_{20}H_{20}$	0.0	0.0	0.0	0.0	4.91	1.01
$Ge_{80}H_{80}$	–2.4	–0.4	–5.8	–3.8	3.61	1.70
$Ge_{180}H_{180}$	–3.3		–7.1		3.59	2.45
$Ge_{320}H_{320}$	–3.9				3.34	3.20
$Ge_{500}H_{500}$	–4.2				3.18	3.97
Series 60m^2						
$Ge_{60}H_{60}$	6.0	8.1	6.7	8.8	4.24	1.54
$Ge_{240}H_{240}$	–0.1				3.54	2.75
GeH sheet	–5.3				2.28	

[a] The energies in kJ/mol per GeH unit are given relative to $Ge_{20}H_{20}$.
[b] Gibbs corrections for total energy obtained from B3LYP calculations.

Table 4. Relative total energies and Gibbs free energies (T = 298.15K),[a] HOMO–LUMO gaps, and diameters of I_h-symmetric polystannanes together with the infinite SnH sheet.

	ΔE_{B3LYP}	ΔG_{B3LYP}	ΔE_{MP2}	ΔG_{MP2}[b]	Gap_{B3LYP} (eV)	Diameter (nm)
Series 20m^2						
$Sn_{20}H_{20}$	0.0	0.0	0.0	0.0	3.55	1.15
$Sn_{80}H_{80}$	–2.6	–1.0	–5.2	–3.6	2.79	1.96
$Sn_{180}H_{180}$	–3.6	–1.6			2.34	2.82
$Sn_{320}H_{320}$	–4.1				2.03	3.70
$Sn_{500}H_{500}$	–4.4				1.82	4.59
Series 60m^2						
$Sn_{60}H_{60}$	3.3	5.1	5.0	6.7	3.21	1.77
$Sn_{240}H_{240}$	–1.2				2.47	3.18
SnH sheet	–5.4				0.94	

[a] The energies in kJ/mol per SnH unit are given relative to $Sn_{20}H_{20}$.
[b] Gibbs corrections for total energy obtained from B3LYP calculations.

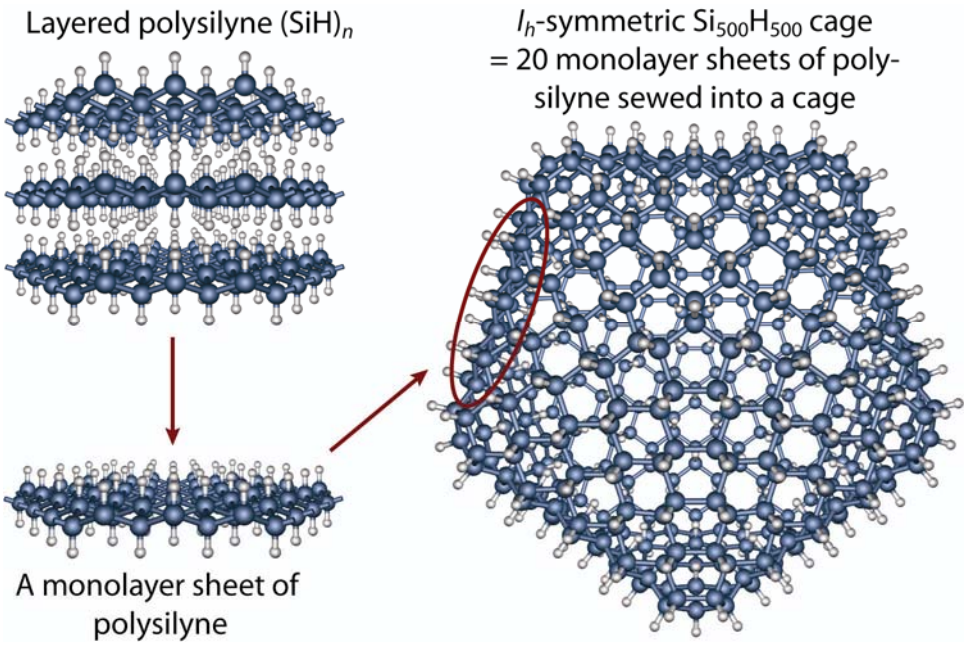

Figure 11. The structural relation between the experimentally known layered polysilyne and the I_h-symmetric polysilanes. The same logic applies for the experimentally known layered polygermyne, $(GeH)_n$, and I_h-symmetric polygermanes.

The structural relation between the icosahedral $(MH)_n$ cages and corresponding infinite, strain-free monolayer sheets allows estimation of the strain energies of the cages. The energy difference between a cage and the corresponding monolayer sheet can be considered as the strain energy resulting from the curvature of the cage. The largest studied cages of the $20m^2$ series, $Si_{500}H_{500}$, $Ge_{500}H_{500}$, and $Sn_{500}H_{500}$, have B3LYP strain energies of only 1.0, 1.1, and 1.0 kJ/mol per MH unit, respectively. For comparison, the strain energy of the C_{60} fullerene is about 40 kJ/mol per C atom at the same level of theory.[71] Multilayered icosahedral cages can be derived by placing smaller cages inside the larger ones. Looking at the more stable $20m^2$ series of structures, the mth member of the series can be fit inside the $(m+2)$th member, the first feasible multilayered cages thus being $M_{20}H_{20}@M_{180}H_{180}$ and $M_{80}H_{80}@M_{320}H_{320}$.

Polysilanes, polygermanes, and polystannanes can be produced experimentally by several techniques. Polysilanes have been synthesized by Wurtz-type coupling of dichlorosilanes, transition metal catalyzed polymerizations, and ultrasonic activation.[6] The transition metal catalysis and ultrasound activation techniques can also be used to prepare polygermanes and polystannanes.[7] Furthermore, small $(SiH)_n$ cages up to n = 22 have been synthesized by laser photolysis.[72] The preparation of the icosahedral group 14 $(MH)_n$ cages might require completely novel experimental approaches, but the various existing synthetic methods can offer helpful guidelines.

4.2. ELECTRONIC PROPERTIES

The electronic properties of the icosahedral group 14 $(MH)_n$ cages can be studied by investigating the HOMO–LUMO gaps of the cages and band gaps of the periodic $(MH)_n$ reference structures. The H–L gaps of hydrated Si,[73] Ge,[74] and Si–Ge[75] nanocrystals have been shown to correlate well with optical gaps predicted by time-dependent DFT methods. For the studied $(SiH)_n$, $(GeH)_n$, and $(SnH)_n$ cages, the H–L gaps approach the direct band gaps calculated for the layered polysilyne, GeH monolayer, and SnH monolayer, respectively (Tables 2–4). Previous theoretical studies[19] indicate a direct band gap of about 3 eV for the layered polysilyne, and experimental photoluminescence data suggests a direct optical gap at around 2.2 eV.[76] According to photoluminescence measurements[18] and theoretical calculations,[20] the layered polygermyne possesses a direct band gap of 1.7 eV. Comparisons of the electronic properties of the icosahedral $(MH)_n$ cages and the corresponding periodic $(MH)_n$ reference structures suggest that the predicted cages possess useful optical properties, such as efficient luminescence.

The calculated H–L gaps of the $(SiH)_n$, $(GeH)_n$, and $(SnH)_n$ cages decrease systematically in the order Si > Ge > Sn. Thus, preparation of mixed group 14 cages such as $Si_{n-x}Ge_xH_n$, with control over x, would enable engineering of the optical gap. Si and Ge are known to be completely miscible, and Si–Ge network[16] and sheet[77] polymers with tuneable luminescence have already been produced. Experimental syntheses of group 14 $(MH)_n$ cages and their mixed or multilayered combinations could, therefore, lead to nanostructures with tuneable optical properties.

5. ICOSAHEDRAL AND RING-SHAPED ALLOTROPES OF PHOSPHORUS AND ARSENIC[III, V]

5.1. ICOSAHEDRAL ALLOTROPES

Phosphorus and arsenic have small polyhedral allotropes, the white phosphorus, P_4,[22] and yellow arsenic, As_4.[30] However, structurally characterized larger polyhedral allotropes have not been prepared so far. The smallest icosahedral phosphorus cage, the P_{20} dodecahedron (Figure 12), has been theoretically shown to be unstable with respect to dissociation into P_4.[78] In contrast to P_{20}, the corresponding I_h-symmetric As_{20} cage is energetically comparable to As_4,[79] having also been synthesized as the outer shell of the $[As@Ni_{12}@As_{20}]^{3-}$ ion.[80] The larger I_h-symmetric cages, P_{60}[81] and As_{60},[79b] analogous to the C_{60} fullerene, are unstable with respect to P_4 and As_4. The planarity of the 60-membered cage results in serious structural strain due to the increased lone pair repulsions (Figure 12). Therefore, larger and increasingly planar polyhedral cages with all lone pairs pointing outwards are expected to be structurally strained. However, in the case of larger I_h-symmetric phosphorus and arsenic cages, the lone pair repulsion can be decreased by placing a portion of the lone pairs inside the cage. As in the case of icosahedral fulleranes[I] and heavier group 14 cages,[II,IV] this in–out isomerism is applicable from the 80-membered cage onwards. In the icosahedral P_{80} and As_{80} cages, the 20 atoms interconnecting each set of three pentagons can be directed toward the cage center, resulting in a puckered structure (Figure 12). Placing the 20 lone pairs inside the cage has a significant stabilizing effect on the icosahedral cages, both P_{80} and As_{80} being noticeably more stable than white phosphorus or yellow arsenic in terms of B3LYP and MP2 total energies (Tables 5 and 6).

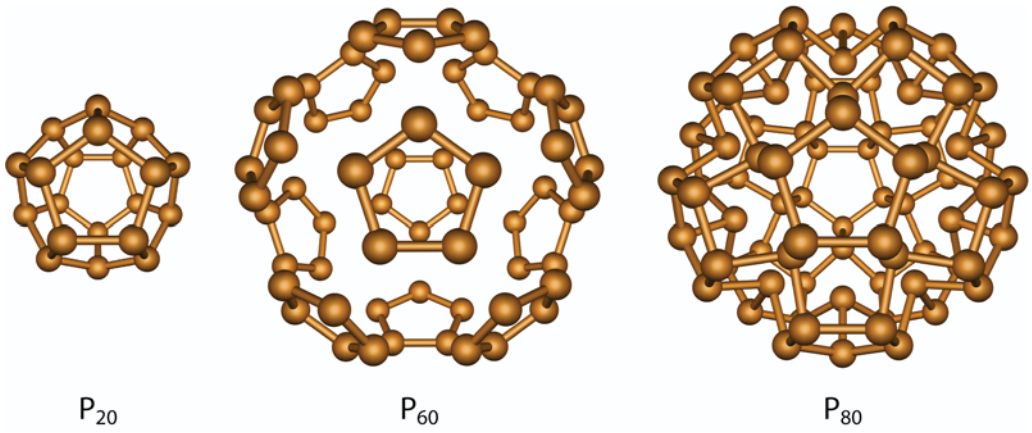

Figure 12. The three smallest I_h-symmetric phosphorus cages. The P_{60} cage with several imaginary vibrational frequencies is not a true minimum structure. The corresponding icosahedral allotropes of arsenic are structurally equivalent to the phosphorus cages.

Table 5. Relative total energies, Gibbs free energies (T = 298.15 K),[a] HOMO-LUMO gaps, and diameters of the icosahedral cages of phosphorus together with the monolayer sheet of rhombohedral black phosphorus.

	Point group	ΔE_{B3LYP}	ΔG_{B3LYP}	ΔE_{MP2}	ΔG_{MP2}[b]	Gap_{B3LYP} (eV)	Diameter (nm)
P_4	T_d	0.0	0.0	0.0	0.0	6.48	
P_{20}	I_h	2.26	13.5	4.10	15.3	2.93	0.6
P_{80}	I_h	–6.72	6.95	–10.4	3.20	2.79	1.2
P_{180}	I_h	–9.65	4.60	–14.1	0.15	2.53	1.8
P_{320}	I_h	–11.3		–15.9		2.77	2.4
P_{500}	I_h	–12.4				2.83	3.1
P_{720}	I_h	–13.2				2.75	3.7
$P_{r\text{-}sheet}$		–16.6				3.41	

[a] The energies in kJ/mol per phosphorus atom are given relative to the white phosphorus, P_4.
[b] Gibbs corrections to the total energies obtained from the B3LYP calculations.

Table 6. Relative total energies, Gibbs free energies (T = 298.15 K),[a] HOMO-LUMO gaps, and diameters of the icosahedral cages of arsenic together with the monolayer sheet of rhombohedral gray arsenic.

	Point group	ΔE_{B3LYP}	ΔG_{B3LYP}	ΔE_{MP2}	ΔG_{MP2}[b]	Gap_{B3LYP} (eV)	Diameter (nm)
As_4	T_d	0.0	0.0	0.0	0.0	5.46	
As_{20}	I_h	–1.8	9.7	–3.2	8.3	2.66	0.7
As_{80}	I_h	–7.1	6.5	–18.7	–5.1	2.42	1.3
As_{180}	I_h	–9.4	4.6	–22.7	–8.6	2.40	2.0
As_{320}	I_h	–10.7				2.59	2.7
As_{500}	I_h	–11.6				2.57	3.4
$As_{r\text{-}sheet}$		–15.4				3.08	

[a] The energies in kJ/mol per arsenic atom are given relative to the yellow arsenic, As_4.
[b] Gibbs corrections to the total energies obtained from the B3LYP calculations.

Applying the in–out isomeric structural motif to larger I_h-symmetric phosphorus and arsenic cages produces two distinct series of structures with different ring topologies. The next I_h-symmetric cage, the 180-membered puckered icosahedron with 60 lone pairs inside the cage, belongs to a series where the cages are composed of 12 pentagons and an increasing number of puckered hexagons (Figure 13). The next cage after the 180-membered icosahedron, the 240-membered cage (Figure 14), is an extension of the

60-membered cage, belonging to a series of cages composed of 12 pentagons, 20 planar hexagons, and an increasing number of puckered hexagons.

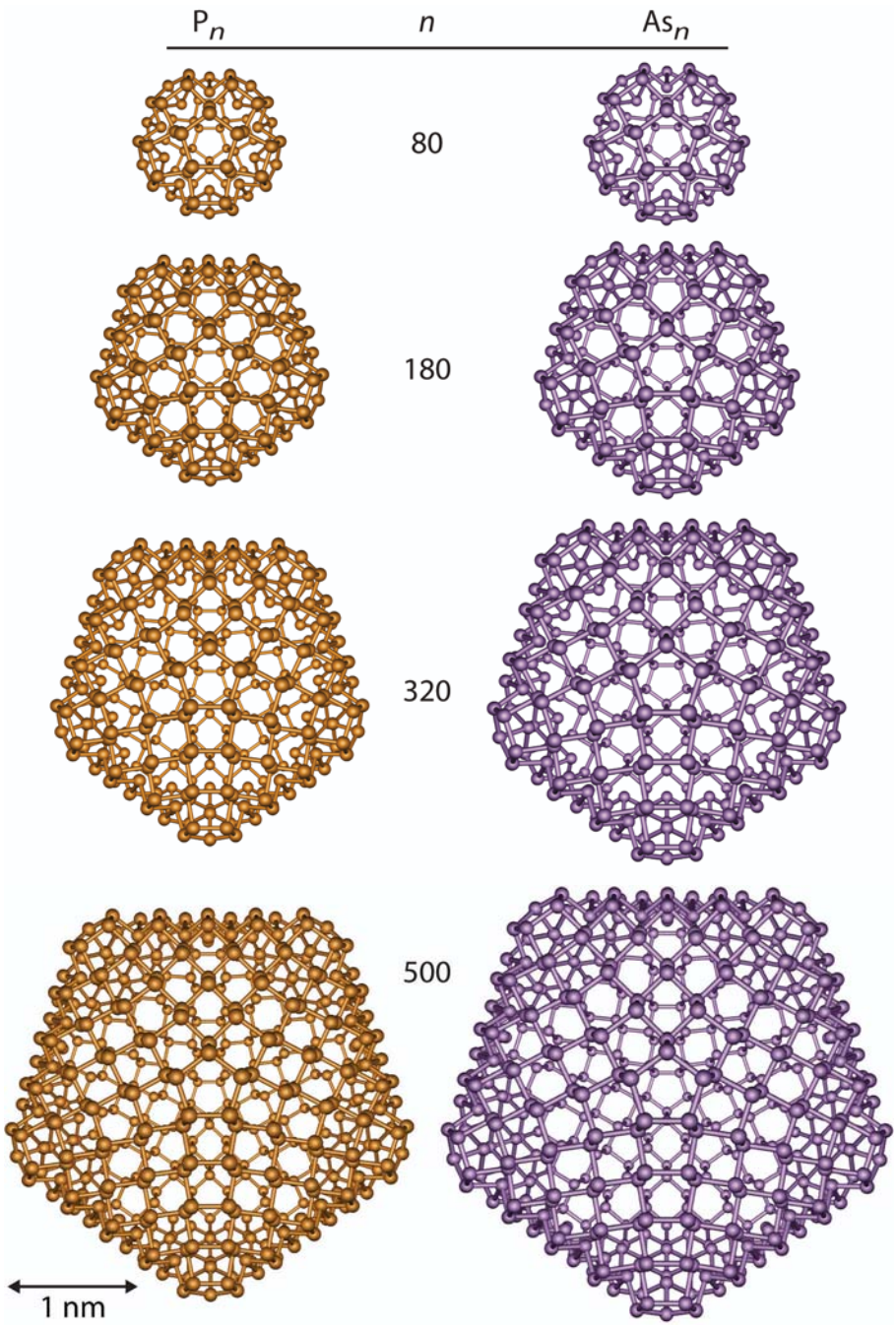

Figure 13. I_h-symmetric allotropes of phosphorus and arsenic belonging to the $n = 20m^2$ series of structures, with $m = 2–5$.

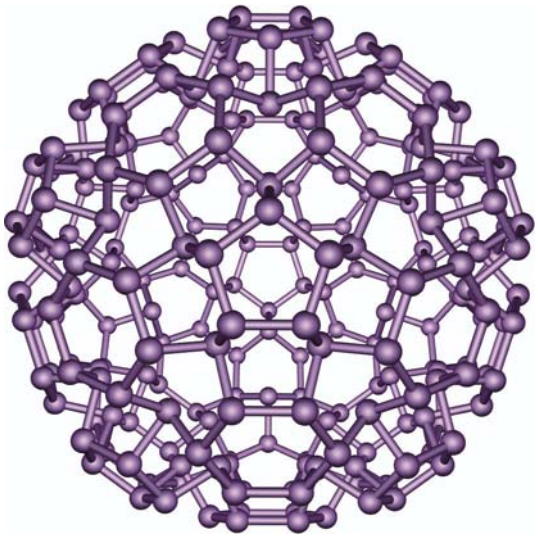

Figure 14. I_h-symmetric As_{240} cage belonging to the $n = 60m^2$ series of structures.

The members of the two series of icosahedral P_n and As_n cages can be derived from the two simple formulas introduced for the icosahedral cages of group 14:[II,IV] (1) n = 20, 80, 180, 320, 500, …, $20m^2$ and (2) n = 60, 240, 540, 960, 1500, …, $60m^2$ (m = 1, 2, 3, …). As in the case of the in–out isomeric group 14 cages, the $20m^2$ and $60m^2$ structural series of I_h-symmetric P_n and As_n allotropes have ring topologies analogous to those of the icosahedral (h,0) and (h,k), h=k fullerenes, respectively.[70] The $60m^2$ series is less stable due to the lone pair repulsion associated with the planar hexagons. Furthermore, P_{60}, P_{240}, and As_{60} cages are not true minimum structures, all having several imaginary vibrational modes. The following discussion of the icosahedral allotropes of phosphorus and arsenic is accordingly focused on the more stable $20m^2$ series of structures.

The members of the $20m^2$ series become increasingly stable as a function of the size of the cage (Tables 5 and 6). As the icosahedral allotropes become larger, they adopt clearly faceted shapes, each of the 20 facets resembling a monolayer of rhombohedral black phosphorus or gray arsenic (Figure 15). As a consequence, the relative total energies of the phosphorus and arsenic cages approach the energies calculated for the corresponding monolayer sheets of black phosphorus and gray arsenic (Tables 5 and 6). Considering the monolayer sheets as strain-free reference systems, the energy difference between each cage and the corresponding phosphorus or arsenic sheet can be defined as the strain energy of the cage. The strain energies of the largest calculated icosahedral P_{720} and As_{500} cages are 3.4 and 3.8 kJ/mol per atom, respectively. In comparison with the strain energy of about 40 kJ/mol per atom calculated for the C_{60} fullerene,[71] the strain energies of phosphorus and arsenic cages are small.

Gibbs free energy corrections to the calculated total energies do not change the observed energy trends (Tables 5 and 6). However, according to the B3LYP results, the smaller phosphorus and arsenic cages become less stable than P_4 or As_4 at 298.15 K. At

the MP2 level of theory, the phosphorus cages from P_{320} on are expected to be thermodynamically more stable than P_4, whereas the arsenic cages are already thermodynamically favored over As_4 from As_{80} onwards.

The calculated HOMO–LUMO gaps of the cages do not exhibit any systematic trends, fluctuations being found for both phosphorus and arsenic cages (Tables 5 and 6). The gaps of the phosphorus cages vary between 2.53 and 2.93 eV, while the calculated band gap of the corresponding monolayer sheet of rhombohedral black phosphorus is 3.41 eV. Similarly, the HOMO–LUMO gaps of the arsenic cages vary between 2.40 and 2.66 eV, while the value for the monolayer sheet of rhombohedral gray arsenic is 3.08 eV.

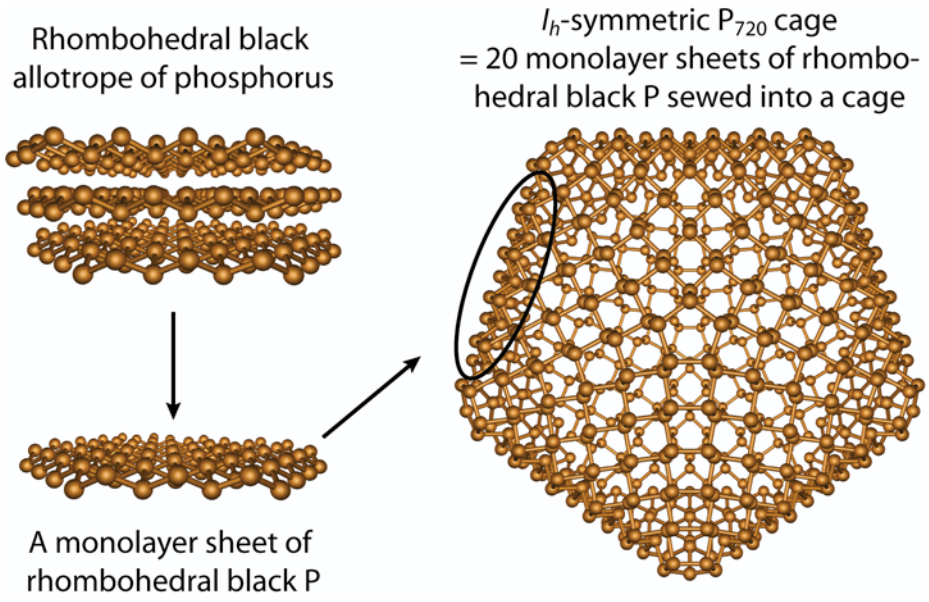

Figure 15. The structural relation between the rhombohedral black phosphorus and the I_h-symmetric allotropes of phosphorus. The same logic applies for the rhombohedral gray arsenic and I_h-symmetric arsenic cages.

5.2. RING-SHAPED ALLOTROPES

The ring-shaped allotropes of phosphorus and arsenic can be derived from structural motifs related to those of the red allotrope of phosphorus, which is known to form various chain-like modifications.[28,82] Short C_{2v}-symmetric 18- and 28-membered chains composed of 8 + 2 atom subunits have been found to be stable clusters of red phosphorus[78] (Figure 16). Incremental addition of 8 + 2 atom subunits to the short C_{2v}-symmetric chains results in bent chains (Figure 16), which become increasingly stable as a function of their length. The bent P_{78} and As_{78} chains are already 17.5 and 14.0

kJ/mol per atom more stable at B3LYP level than the corresponding P_4 and As_4 allotropes. Addition of a two-atom fragment between the terminal subunits enables closure of the 78-membered chain, yielding a ring-shaped 80-membered chain (Figure 17). The 80-membered rings are slightly strained due to lone pair repulsion inside the ring, causing the 8-atom subunits to twist out of the ring plane. The resulting C_{4v}-symmetric P_{80} and As_{80} rings are the smallest true minimum ring structures. Use of higher C_{8v} or D_{8h} symmetries for the 80-membered rings results in structures with several imaginary vibrational modes.

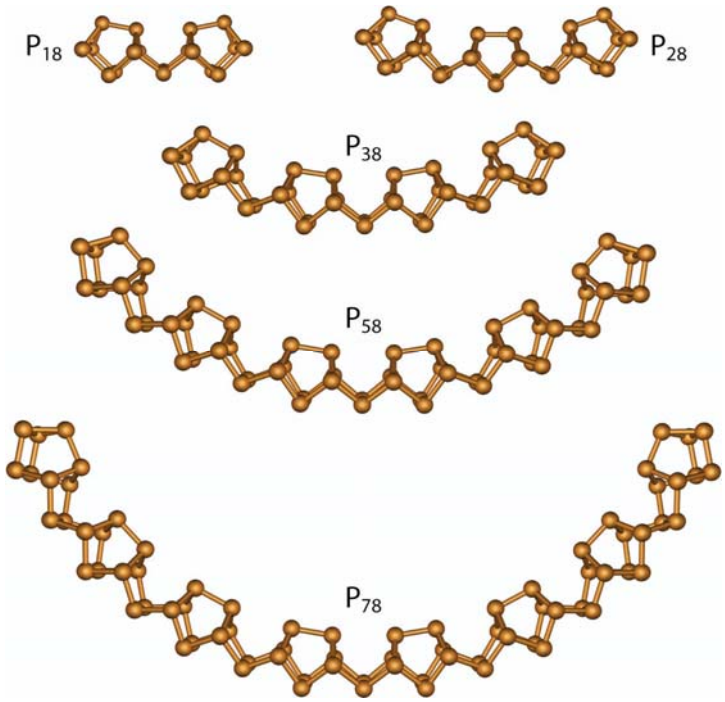

Figure 16. The optimized structures of C_{2v}-symmetric bent phosphorus chains composed of P_8 and P_2 structural subunits.

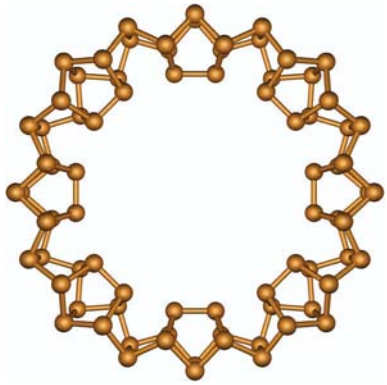

Figure 17. C_{4v}-symmetric, ring-shaped P_{80} allotrope of phosphorus.

The structural strain present in the 80-membered ring can be decreased by increasing the size of the ring. Considering larger rings that can be derived by incremental additions of four 8 + 2 atom units, the next ring is 120-membered. Here the lone pair repulsion inside the ring is significantly smaller than for the 80-membered ring, allowing a completely planar orientation and D_{12h} symmetry (Figure 18).[83] The P_{120} and As_{120} rings are noticeably more stable than the P_{80} and As_{80} rings, with both 80- and 120-membered rings clearly favored over P_4 and As_4 in terms of B3LYP and MP2 total energies (Tables 7 and 8).

The stability of the ring-shaped chains peaks around 200 atoms for both phosphorus and arsenic, after which the stabilities slowly decrease (Tables 7 and 8). The curvature of the rings decreases as a function of their size, converging toward a linear chain composed of 8 + 2 atom units. Using the naming convention originally devised for phosphorus chains by Böcker and Häser,[82] the infinite chain composed of 8 + 2 atom units can be denoted as]X2[X8], where X = P or As. Several infinite chains of red phosphorus are shown in Figure 19. All the studied phosphorus and arsenic rings except P_{80} and As_{80} are more stable than the corresponding infinite]P2[P8] and]As2[As8] chains (Tables 7 and 8), demonstrating the favorable effect of chain bending. Consideration of the Gibbs free energies at 298.15 K does not alter the observed energy trends, though the P_{80} and As_{80} rings are less stable than P_4 and As_4 in terms of B3LYP Gibbs free energies. The ring-shaped allotropes of phosphorus are practically equal in stability to the experimentally known fibrous red and violet phosphorus (Table 7), suggesting the possibility of preparing the ring-shaped chains. However, being three-dimensional solid-state structures, the fibrous red and violet allotropes probably can adopt a more compact crystal packing than the rings.

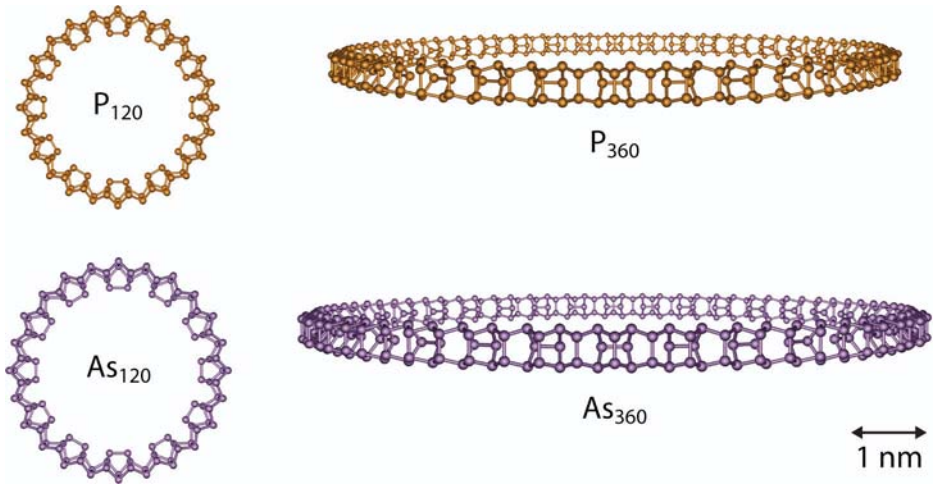

Figure 18. Ring-shaped allotropes of phosphorus and arsenic: top view of the 120-membered rings and side view of the 360-membered rings.

Table 7. Relative total energies, Gibbs free energies (T = 298.15 K),[a] HOMO-LUMO gaps, and diameters of the ring-shaped chains of phosphorus together with other forms of phosphorus.[b]

	Point group	ΔE_{B3LYP}	ΔG_{B3LYP}	ΔE_{MP2}	ΔG_{MP2}[c]	Gap_{B3LYP} (eV)	Diameter (nm)
P_4	T_d	0.0	0.0	0.0	0.0	6.48	
P_{80}	C_{4v}	–13.3	0.25	–17.3	–3.61	3.13	1.9
P_{120}	D_{12h}	–17.9	–4.00	–21.1	–7.17	3.53	2.7
P_{160}	D_{16h}	–18.7	–4.66	–21.6	–7.61	3.58	3.5
P_{200}	D_{20h}	–18.8	–4.73	–21.6	–7.57	3.60	4.4
P_{240}	D_{24h}	–18.7	–4.68	–21.5	–7.45	3.62	5.2
P_{280}	D_{28h}	–18.6	–4.59	–21.3	–7.33	3.64	6.0
P_{320}	D_{32h}	–18.5		–21.2		3.65	6.9
P_{360}	D_{36h}	–18.4				3.66	7.7
]P2[P8]		–17.2				3.63	
]P4(4)[P8]		–17.0				3.67	
]P2[P10]		–16.9				3.43	
]P2[P12(4)]		–16.4				3.65	
$P_{fibrous}$		–18.7				2.73	
P_{violet}		–19.1				2.56	

[a] The energies in kJ/mol per phosphorus atom are given relative to the white phosphorus P_4.
[b] The following forms are included: infinite chains of red phosphorus,]P2[P8],]P4(4)[P8],]P2[P10], and]P2[P12(4)] (Figure 19); fibrous red phosphorus, $P_{fibrous}$; violet phosphorus, P_{violet}.
[c] Gibbs corrections to the total energies obtained from the B3LYP calculations.

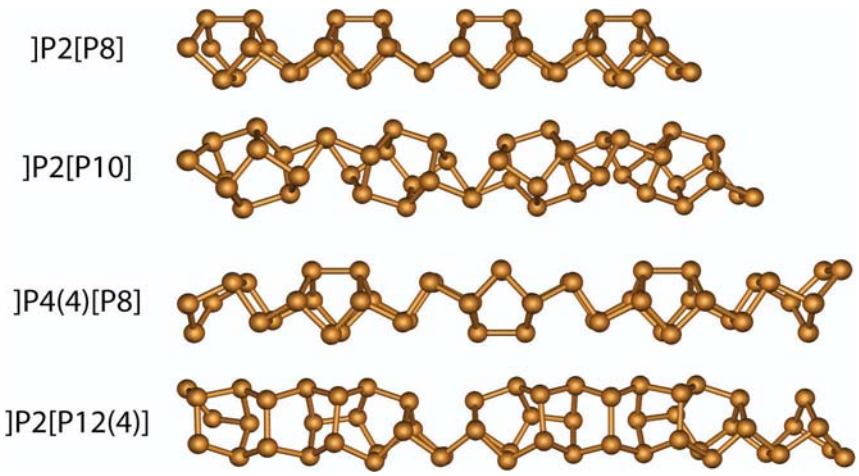

Figure 19. Various infinite chains of phosphorus.

Table 8. Relative total energies, Gibbs free energies (T = 298.15 K),[a] HOMO-LUMO gaps, and diameters of the ring-shaped chains of arsenic together with infinite chains of arsenic.[b]

	Point group	ΔE_{B3LYP}	ΔG_{B3LYP}	ΔE_{MP2}	ΔG_{MP2}[c]	Gap_{B3LYP} (eV)	Diameter (nm)
As_4	T_d	0.0	0.0	0.0	0.0	5.46	
As_{80}	C_{4v}	–11.2	2.1	–21.3	–8.0	2.46	2.1
As_{120}	D_{12h}	–14.4	–0.9	–24.0	–10.4	2.92	3.0
As_{160}	D_{16h}	–14.9	–1.3	–24.1	–10.5	3.02	3.9
As_{200}	D_{20h}	–14.9		–23.9		3.07	4.8
As_{240}	D_{24h}	–14.9				3.06	5.7
As_{280}	D_{28h}	–14.8				3.06	6.6
As_{320}	D_{32h}	–14.7				3.05	7.5
As_{360}	D_{36h}	–14.6				3.05	8.4
]As2[As8]		–13.9				3.01	
]As4(4)[As8]		–13.5				3.10	
]As2[As10]		–14.0				2.94	
]As2[As12(4)]		–13.5				3.14	

[a] The energies in kJ/mol per arsenic atom are given relative to the yellow arsenic As_4.
[b] The following infinite chains of arsenic are included:]As2[As8],]As4(4)[As8],]As2[As10], and]As2[As12(4)]. The chains are analogous to the phosphorus chains in Figure 19.
[c] Gibbs corrections to the total energies obtained from the B3LYP calculations.

The calculated HOMO–LUMO gaps of the ring-shaped allotropes behave differently for phosphorus and arsenic. For phosphorus, the gaps increase slowly at least up to P_{360}. The sizes of the gaps are about 3.6 eV and close to the band gap calculated for the infinite]P2[P8] chain. In the case of arsenic, the gap size reaches a maximum at As_{200}, after which it slowly begins to decrease. The HOMO–LUMO gaps of the rings and the band gap of the corresponding infinite chain are nearly equal for arsenic, as well.

5.3. COMPARISONS OF THE ALLOTROPES

Comparisons of the allotropes of phosphorus and arsenic reveal distinct differences in the two elements. The relative B3LYP total energies of the various allotropes of phosphorus are compared in Figure 20, and the corresponding values for arsenic are presented in Figure 21. For phosphorus, all the studied ring-shaped structures are favored over the icosahedral cages. As the number of phosphorus atoms increases beyond 200, the stability of the rings slowly begins to decrease towards the linear]P2[P8] chain, while the stability of the cages approaches that of the monolayer sheet

of rhombohedral black phosphorus. The relative energy difference between the chain and sheet is 0.53 kJ/mol per atom in favor of the chain. In the case of arsenic, the cages are expected to surpass the rings in stability since the monolayer sheet of rhombohedral gray arsenic is 1.5 kJ/mol per atom more stable than the infinite]As2[As8] chain. The preference of arsenic for cages is understandable, as the rhombohedral gray allotrope is the most stable allotrope of arsenic at standard temperature and pressure,[30] while the formation of rhombohedral black phosphorus requires high pressures.[25]

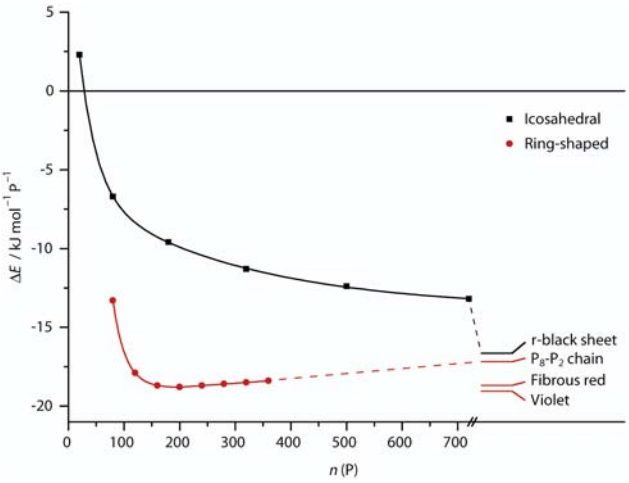

Figure 20. B3LYP total energies of the allotropes of phosphorus relative to the white phosphorus, P_4. The reference allotropes on the right are a monolayer sheet of the rhombohedral black phosphorus, an infinite]P2[P8] chain, fibrous red phosphorus, and violet phosphorus.

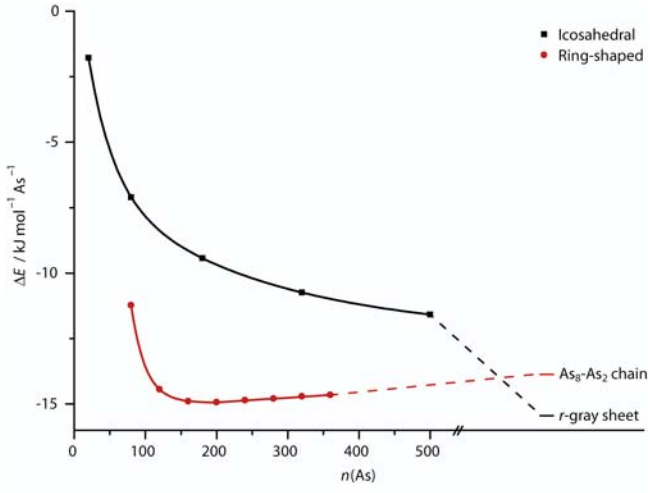

Figure 21. B3LYP total energies of the allotropes of arsenic relative to the yellow arsenic, As_4. The reference allotropes on the right are an infinite]As2[As8] chain and a monolayer sheet of the rhombohedral gray arsenic.

In view of the differences in thermodynamic stabilities of the cages and rings for phosphorus and arsenic, it would be reasonable to focus possible experimental efforts first on phosphorus rings or arsenic cages. The ring-shaped chains or icosahedral cages would probably be obtainable at intermediate temperatures, as very high temperature syntheses would more likely favor the formation of P_4 or As_4.

The copper–halide matrix techniques used to produce various phosphorus[28] and mixed P–As chains[33] might offer synthetic pathways to the ring-shaped chains. Another possibility is the variation of crystallization catalysts and conditions, as in the recent synthesis of the fibrous red phosphorus.[27] Whereas the violet phosphorus can be crystallized from lead melt, the preparation of the fibrous red phosphorus required the presence of a iodine catalyst.

In the case of cages, one experimental route to larger icosahedral cages could be the synthetic techniques used in the preparation of the As_{20} cage incorporated in the $[As@Ni_{12}@As_{20}]^{3-}$ ion.[80] Stabilizing the cages through use of larger endohedral metal cages than Ni_{12} might be one possibility. An entirely different synthetic approach might be derived from the analogy between the cages composed of monolayer sheets and fullerenes formed from graphene sheets. Several methods are known to efficiently produce icosahedral fullerenes from graphite.[84] Multiwalled phosphorus or arsenic cages could be derived by placing smaller cages inside the larger ones. They would be structurally related to the layered crystal structure of the rhombohedral black phosphorus or gray arsenic. As in the case of icosahedral hydrides of group 14,[II,IV] the mth member of the $20m^2$ structural series could be fit inside the $(m+2)$th member, the two smallest multilayered cages thus being $X_{20}@X_{180}$ and $X_{80}@X_{320}$.

6. SUMMARY

The structures, stabilities, and electronic properties of icosahedral fulleranes, polysilanes, polygermanes, and polystannanes, together with elemental nanostructures of phosphorus and arsenic, were studied by using quantum chemical methods.

Full hydrogenation of icosahedral C_{80} and C_{180} fullerenes, using the novel structural motif of partial endo-hydrogenation, was shown to result in remarkably stable $C_{80}H_{80}$ and $C_{180}H_{180}$ fulleranes. The calculated IR spectra of the fulleranes exhibit vibrational modes similar to unidentified astronomical emission features, suggesting the existence of fulleranes in the interstellar medium. Controlled synthesis of the fulleranes and their further functionalization could open up an entirely new branch of hydrocarbon nanochemistry.

The existence of stable I_h-symmetric families of polysilane, polygermane, and polystannane nanostructures was predicted. The structures were derived using the structural motif of in–out isomerism analogous to that used for the icosahedral fulleranes. The structures, stabilities, and electronic properties of the $(SiH)_n$, $(GeH)_n$, and $(SnH)_n$ cages converge toward the corresponding experimentally known group 14 polymers. The similarities between the icosahedral cages and experimentally known inorganic group 14 polymers with efficient luminescence suggest potential optoelectronic applications for the cages. The preparation of mixed or multilayered combinations of the cages could result in materials with tuneable optical properties

Two new allotropic forms of phosphorus and arsenic were predicted: icosahedral cages and ring-shaped chains. The icosahedral cages are stabilized by minimization of the lone pair repulsions through puckering of the cages, resulting in structures related to black phosphorus and gray arsenic. The ring-shaped allotropes, derived from concatenation of 8 + 2 atom structural units, are structurally related to the red allotrope of phosphorus. Comparisons of the predicted and experimentally known allotropes show the cages and rings to be thermodynamically stable with respect to the white and yellow allotropes of phosphorus and arsenic. The structures and stabilities of the cages approach those of monolayer sheets of rhombohedral black phosphorus and gray arsenic, while the stabilities of the rings peak at around 200 atoms. The phosphorus rings are more stable than the icosahedral cages, being energetically comparable to the experimentally known violet and fibrous red allotropes of phosphorus. In contrast to phosphorus, large icosahedral cages of arsenic are expected to surpass arsenic rings in stability. Controlled synthesis of the icosahedral and ring-shaped allotropes of phosphorus and arsenic would produce elemental nanostructures with well-defined molecular structures.

ACKNOWLEDGMENTS

This work was carried out during the years 2005-2007 at the Department of Chemistry, University of Joensuu. Financial support from the Inorganic Materials Chemistry Graduate program (EMTKO) and Academy of Finland is gratefully acknowledged. I'd also like to thank Hexion Specialty Chemicals for granting me their annual award for chemistry students in the year 2006.

I am most grateful to my supervisor, Professor Tapani Pakkanen, for introducing me to theoretical physical chemistry and providing endless encouragement and first-class resources for scientific work. During my studies I have had the opportunity to participate in numerous interesting and rewarding projects. I sincerely thank Docent Mikko Linnolahti for familiarizing me in the challenging field of computational nanochemistry. Our collaboration has been truly fruitful and incredibly exciting. During our efforts I have also begun to understand the importance of high-quality coffee breaks in the scientific research process.

Dr. Kathleen Ahonen is thanked for revising the language of this dissertation.

The students and staff of the Department of Chemistry have provided a pleasant and friendly working environment. Special thanks go to all people populating the (in)famous Café Luola day after day. The chores in the service of the student organization Bunsen acted as the best possible counterbalance to my studies, and I am grateful for all my friends at the Department of Chemistry for making the university studies such a social and delightful activity. My special thanks go to a good friend, office mate, and gym champion Jukka Tanskanen. Our scientific conversations and deep societal analyses have always been refreshing, not to mention the less formal discussions.

I wish to thank my family for their essential support during my studies. Visits to home at Ylämylly have always been very important for me.

My warmest thanks go to my wife Virve for her love and support. Very often only a chemist can understand what goes in the mind of another chemist.

Joensuu, May 2007 Antti Karttunen

REFERENCES AND NOTES

[1] Kroto, H. W.; Heath, J. R.; O'Brien, S. C.; Curl, R. F.; Smalley, R E. *Nature* **1985**, *318*, 162.

[2] Krätschmer, W.; Lamb, L. D.; Fostiropoulos, K.; Huffman, D. R. *Nature* **1990**, *347*, 354.

[3] Nossal, J.; Saini, R. K.; Alemany, L. B.; Meier, M.; Billups, W. E. *Eur. J. Org. Chem.* **2001**, 4167.

[4] Geballe, T. R.; Tielens, A. G. G. M.; Allamandola, L. J.; Moorhouse, A.; Brand, P. W. J. L. *Astrophys. J.* **1989**, *341*, 278.

[5] Webster, A. *Nature* **1991**, *352*, 412.

[6] Miller, R. D.; Michl, J. *Chem. Rev.* **1989**, *89*, 1359.

[7] Manners, I.; *Angew. Chem. Int. Ed.* **1996**, *35*, 1602.

[8] Wiberg, N.; Finger, C. M. M.; Polborn, K. *Angew. Chem. Int. Ed.* **1993**, *32*, 1054.

[9] Sekiguchi, A.; Nagase, S.; in *The Chemistry of Organic Silicon Compounds*, Vol. 2; Rappoport, Z.; Apeloig, Y.; Eds.; John Wiley & Sons, New York, 1998, pp. 119–152.

[10] (a) Sekiguchi, A.; Yatabe, T.; Kabuto, C.; Sakurai, H. *J. Am. Chem. Soc.* **1993**, *115*, 5853. (b) Sekiguchi, A.; Kabuto, C.; Sakurai, H. *Angew. Chem. Int. Ed.* **1989**, *28*, 55.

[11] (a) Furukawa, K.; Fujino, M.; Matsumoto, N. *Appl. Phys. Lett.* **1992**, *60*, 2744. (b) Sekiguchi, A.; Yatabe, T.; Katamani, H.; Kabuto, C.; Sakurai, H. *J. Am. Chem. Soc.* **1992**, *114*, 6260. (c) Sita, L. R.; Kinoshita, I. *Organometallics* **1990**, *9*, 2865.

[12] Nagase, S. *Acc. Chem. Res.* **1995**, *28*, 469.

[13] Earley, C. W. *J. Phys. Chem. A* **2000**, *104*, 6622.

[14] Sita, L. R. *Acc. Chem. Res.* **1994**, *27*, 191.

[15] Bianconi, P. A.; Weidman, T. W. *J. Am. Chem. Soc.* **1988**, *110*, 2342.

[16] Szymanski, W. J.; Visscher, G. T.; Bianconi, P. A. *Macromolecules* **1993**, *26*, 869.

[17] Dahn, J. R.; Way, B. M.; Fuller, E.; Tse, J. S. *Phys. Rev. B* **1993**, *48*, 17872.

[18] Vogg, G.; Brandt, M. S.; Stutzmann, M. *Adv. Mater.* **2000**, *12*, 1278.

[19] Tse, J. S.; Dahn, J. R.; Buda, F. *J. Phys. Chem.* **1995**, *99*, 1896.

[20] Hajnal, Z.; Vogg, G.; Meyer, L. J.-P.; Szűcs, B.; Brandt, M. S.; Frauenheim, T. *Phys. Rev. B.* **2001**, *64*, 033311.

[21] Nešpůrek, S.; Wang, G.; Yoshino, K. *J. Optoelectron. Adv. Mater.* **2005**, *7*, 223.

[22] Greenwood, N. N.; Earnshaw, A.; in *Chemistry of the Elements*, Butterworth-Heineman, Oxford, **1997**, pp. 479–482.

[23] (a) Corbridge, D. E. C.; Lowe, E. J. *Nature*, **1952**, *170*, 629. (b) Simon, A.; Borrmann, H.; Craubner, H. *Phosphorus Sulfur* **1987**, *30*, 507.

[24] (a) Hultgren, R.; Gingrich, N. S.; Warren, B. E. *J. Chem. Phys.* **1935**, *3*, 351. (b) Brown, A.; Rundqvist, S. *Acta Cryst.* **1965**, *19*, 684.

[25] (a) Jamieson, J. C. *Science* **1963**, *139*, 1291. (b) Kikegawa, T.; Iwasaki, H. *Acta Cryst. B* **1983**, *39*, 158.

[26] Thurn, V. T.; Krebs, U. *Acta Cryst. B.* **1969**, *25*, 125.

[27] Ruck, M.; Hoppe, D.; Wahl, B.; Simon, P.; Wang, Y.; Seifert, G. *Angew. Chem. Int. Ed.* **2005**, *44*, 7616.

[28] (a) Pfitzner, A. *Chem. Eur. J.* **2000**, *6*, 1891. (b) Möller, M. H.; Jeitschko, W. *J. Solid State Chem.* **1986**, *65*, 178. (c) Pfitzner, A.; Freudenthaler, E. *Angew. Chem. Int. Ed.* **1995**, *34*, 1647. (d) Pfitzner, A.; Freudenthaler, E. *Z. Naturforsch. Sect. B* **1997**, *52*, 199.

[29] Pfitzner, A.; Bräu, M. F.; Zweck, J.; Brunklaus, G.; Eckert, H. *Angew. Chem. Int. Ed.* **2004**, *43*, 4228.

[30] Greenwood, N. N.; Earnshaw, A.; in *Chemistry of the Elements*, Butterworth-Heineman, Oxford, **1997**, pp. 550–551.

[31] Schiferl, D.; Barrett, C. S. *J. Appl. Cryst.* **1969**, *2*, 30.

[32] Smith, P. M.; Leadbetter, A. J.; Apling, A. *Philos. Mag.* **1975**, *31*, 57.

[33] (a) Jayasekera, B.; Aitken, J. A.; Heeg, M. J.; Brock, S. L. *Inorg. Chem.* **2003**, *42*, 658. (b) Jayasekera, B.; Brock, S. L.; Lo, A. Y. H.; Schurko, R. W.; Nazri, G-A. *Chem. Eur. J.* **2005**, *11*, 3762.

[34] Jayasekera, B.; Somaskandan, K.; Brock, S. L. *Inorg. Chem.* **2004**, *43*, 6902.

[35] von Schnering, H-G.; Hönle, W. *Chem. Rev.* **1988**, *88*, 243.

[36] Ozin, G. A. *J. Chem. Soc. A* **1970**, 2307.

[37] Shirotani, I.; Mikami, J.; Adachi, T. *Phys. Rev. B* **1994**, *50*, 16274.

[38] (a) Becke, A. D. *J. Chem. Phys.* **1993**, *98*, 5648. (b) Stephens, P. J.; Devlin, F. J.; Chabalowski, C. F.; Frisch, M. J. *J. Chem. Phys.* **1994**, *98*, 11623.

[39] Koch, W. K.; Holthausen, M. C.; in *A Chemist's Guide to Density Functional Theory*, Wiley-VCH, Weinheim, **2000**, pp. 119–148.

[40] TURBOMOLE versions 5.71, 5.8, and 5.9; Ahlrichs, R.; Bär, M.; Häser, M.; Horn, H.; Kölmel, C. *Chem. Phys. Lett.* **1989**, *162*, 165.

[41] Frisch, M. J.; Trucks, G. W.; Schlegel, H. B.; Scuseria, G. E.; Robb, M. A.; Cheeseman, J. R.; Montgomery, Jr., J. A.; Vreven, T.; Kudin, K. N.; Burant, J. C.; Millam, J. M.; Iyengar, S. S.; Tomasi, J.; Barone, V.; Mennucci, B.; Cossi, M.; Scalmani, G.; Rega, N.; Petersson, G. A.; Nakatsuji, H.; Hada, M.; Ehara, M.; Toyota, K.; Fukuda, R.; Hasegawa, J.; Ishida, M.; Nakajima, T.; Honda, Y.; Kitao, O.; Nakai, H.; Klene, M.; Li, X.; Knox, J. E.; Hratchian, H. P.; Cross, J. B.; Bakken, V.; Adamo, C.; Jaramillo, J.; Gomperts, R.; Stratmann, R. E.; Yazyev, O.; Austin, A. J.; Cammi, R.; Pomelli, C.; Ochterski, J. W.; Ayala, P. Y.; Morokuma, K.; Voth, G. A.; Salvador, P.; Dannenberg, J. J.; Zakrzewski, V. G.; Dapprich, S.; Daniels, A. D.; Strain, M. C.; Farkas, O.; Malick, D. K.; Rabuck, A. D.; Raghavachari, K.; Foresman, J. B.; Ortiz, J. V.; Cui, Q.; Baboul, A. G.; Clifford, S.; Cioslowski, J.; Stefanov, B. B.; Liu, G.; Liashenko, A.; Piskorz, P.; Komaromi, I.; Martin, R. L.; Fox, D. J.; Keith, T.; Al-Laham, M. A.; Peng, C. Y.; Nanayakkara, A.; Challacombe, M.; Gill, P. M. W.; Johnson, B.; Chen, W.; Wong, M. W.; Gonzalez, C.; and Pople, J. A. *Gaussian 03*, Revision C.02; Gaussian, Inc.; Wallingford, CT, 2004.

[42] (a) Saunders, V. R.; Dovesi, R.; Roetti, C.; Orlando, R.; Zicovich-Wilson, C. M.; Harrison, N. M.; Doll, K.; Civalleri, B.; Bush, I. J.; D'Arco, Ph. Llunell, M. *CRYSTAL2003 User's Manual*, University of Torino, Torino, Italy, 2003. (b) Dovesi, R.; Saunders, V.R.; Roetti, C.; Orlando, R.; Zicovich-Wilson, C.M.; Pascale, F.; Civalleri, B.; Doll, K.; Harrison, N. M.; Bush, I. J.; D'Arco, Ph.; Llunell, M. *CRYSTAL06 User's Manual*, University of Torino, Torino, Italy, 2006.

[43] Dovesi, R.; Civalleri, B.; Orlando, R.; Roetti, C.; Saunders, V. R.; in *Reviews in Computational Chemistry*, Vol. 21; Lipkowitz, K. B.; Larter, R.; Cundari, T. R.; Eds.; John Wiley & Sons, New York, 2005, pp. 1–125.

[44] Catti, M.; Pavese, A.; Dovesi, R.; Saunders, V. R. *Phys. Rev. B* **1993**, *47*, 9189.

[45] Civalleri, B.; Zicovich-Wilson, C. M.; Ugliengo, P.; Saunders, V. R.; Dovesi, R. *Chem. Phys. Lett.* **1998**, *292*, 394.

[46] Hariharan, P. C.; Pople, J. A. *Theor. Chem. Acc.* **1973**, *28*, 213.

[47] (a) Zicovich-Wilson, C. M.; Bert, A.; Roetti, C.; Dovesi, R.; Saunders, V. R. *J. Chem. Phys.* **2002**, *116*, 1120. (b) CRYSTAL basis set library at http://www.crystal.unito.it

[48] (a) Schaefer, A.; Horn, H.; Ahlrichs, R. *J. Chem. Phys.* **1992**, *97*, 2571. (b) Weigend, F.; Ahlrichs, R. *Phys. Chem. Chem. Phys.* **2005**, *7*, 3297.

[49] Metz, B.; Stoll, H.; Dolg, M. *J. Chem. Phys.* **2000**, *113*, 2563.

[50] Pyykkö, P. *Chem. Rev.* **1988**, *8*8, 563.

[51] (a) Weigend, F.; Häser, M. *Theor. Chem. Acc.* **1997**, *97*, 331. (b) Hättig, C.; Weigend, F. *J. Chem. Phys.* **2000**, *113*, 5154.

[52] Cremer, D.; in *Encyclopedia of Computational Chemisty*; Schleyer, P. von R., Ed.; John Wiley & Sons: New York, 1998; Vol. 3, pp. 1706–1735.

[53] Schäfer, A.; Huber, C.; Ahlrichs, R. *J. Chem. Phys.* **1994**, *100*, 5829.

[54] Weigend, F.; Häser, M.; Patzelt, H.; Ahlrichs, R. *Chem. Phys. Lett.* **1998**, *294*, 143.

[55] Weigend, F.; Ahlrichs, R. *Phys. Chem. Chem. Phys.* **2005**, *7*, 3297.

[56] Hellweg, A.; Hättig, C.; Höfener, S.; Klopper, W. *Theor. Chem. Acc.* **2007**, *117*, 587.

[57] Deglmann, P. ; Furche, F. ; Ahlrichs, R. *Chem. Phys. Lett*. **2002**, *362*, 511.

[58] Scott, A. P.; Radom, L. *J. Phys. Chem.* **1996**, *100*, 16502.

[59] Paquette, L. A.; Ternansky, T. J.; Balogh, D. W.; Kentgen, G. *J. Am. Chem. Soc.* **1983**, *105*, 5446.

[60] Schultz, H. P. *J. Org. Chem.* **1965**, *30*, 1361.

[61] Saunders, M. *Science* **1991**, *253*, 330.

[62] Dodziuk, H.; Nowinski, K. *Chem. Phys. Lett.* **1996**, *249*, 406.

[63] Wu, H-S.; Qin, X-F.; Xu, X-H.; Jiao, H.; Schleyer, P. von R. *J. Am. Chem. Soc.* **2005**, *127*, 2334.

[64] Ruffieux, P.; Gröning, O.; Bielmann, M.; Mauron, P.; Schlapbach, L.; Gröning, P. *Phys. Rev. B* **2002**, *66*, 245416.

[65] (a) Sun, X-H.; Li, C-P.; Wong, N-B.; Lee, C-S.; Lee, S-T.; Teo, B-K. *J. Am. Chem. Soc.* **2002**, *124*, 14856. (b) Li, C. P.; Teo, B-K.; Sun, X. H. Wong, N. B.; Lee, S. T. *Chem. Mater.* **2005**, *17*, 5780.

[66] Kniaź, K.; Fischer, J. E.; Selig, H.; Vaughan, G. B. M.; Romanow, W. J.; Cox, D. M.; Chowdhury, S. K.; McCauley, J. P.; Strongin, R. M.; Smith A. B., *J. Am. Chem. Soc.* **1993**, *115*, 6060.

[67] van Diedenhoven, B.; Peeters, E.; van Kerckhoven, C.; Hony, S.; Hudgins, D. M.; Allamandola, L. J.; Tielens, G. G. M. *Astrophys. J.* **2004**, *611*, 928.

[68] Stoldt, C. R.; Maboudian, R.; Carraro, C. *Astrophys. J.* **2001**, *548*, L225.

[69] Kumar, V.; Kawazoe, Y. *Phys. Rev. Lett.* **2003**, *90*, 055502.

[70] Tang, A. C.; Huang, F. Q. *Chem. Phys. Lett.* **1995**, *247*, 494.

[71] Linnolahti, M.; Kinnunen, N. M.; Pakkanen, T. A. *Chem. Eur. J.* **2006**, *12*, 218.

[72] Rechtsteiner, G. A.; Hampe, O.; Jarrold, M. F. *J. Phys. Chem. B* **2001**, *105*, 4188.

[73] Garoufalis, C. S.; Zdetsis, A. D.; Grimme, S. *Phys. Rev. Lett.* **2001**, *87*, 276402.

[74] Garoufalis, C. S.; Skaperda, M. S.; Zdetsis, A. D. *J. Phys. Conf. Ser.* **2005**, *10*, 97.

[75] Zdetsis, A. D.; Garoufalis, C. S.; Skaperda, M. S.; Koukaras, E. N. *J. Phys. Conf. Ser.* **2005**, *10*, 101.

[76] He, J.; Tse, J. S.; Klug, D. D.; Preston, K. F. *J. Mater. Chem.* **1998**, *8*, 705.

[77] Vogg, G.; Meyer, A. J.-P.; Miesner, C.; Brandt, M. S.; Stutzmann, M. *Appl. Phys. Lett.* **2001**, *78*, 3956.

[78] Häser, M.; Schneider, U.; Ahlrichs, R. *J. Am. Chem. Soc.* **1992**, *114*, 9551.

[79] (a) Shen, M.; Schaefer, H. F. *J. Chem. Phys.* **1994**, *101*, 2261. (b) Baruah, T.; Pederson, M. R.; Zope, R. R.; Beltrán, M. R. *Chem. Phys. Lett.* **2004**, *387*, 476.

[80] Moses, M. J.; Fettinger, J. C.; Eichhorn, B. W. *Science* **2003**, *300*, 778.

[81] Han, J-G.; Morales, J. A. *Chem. Phys. Lett.* **2004**, *396*, 27.

[82] Böcker, S.; Häser, M. *Z. Anorg. Allg. Chem.* **1995**, *621*, 258.

[83] Due to the software imposed limits in the number of real representations per symmetry group, lower symmetries have been used in the calculations for P/As rings: $C_{(x/10)v}$ from X_{120} to X_{160} and $C_{(x/20)v}$ from X_{200} to X_{360}.

[84] (a) Krätschmer, W.; Lamb, L. D.; Fostiropoulos, K.; Huffman, D. R. *Nature* **1990**, *347*, 354. (b) Haufler, R. E.; Conceicao, J.; Chibante, L. P. F.; Chai, Y.; Byrne, N. E.; Flanagan, S.; Haley, M. M.; O'Brien, S. C.; Pan, C.; Xiao, Z.; Billups, W. E.; Ciufolini, M. A.; Hauge, R. H.; Margrave, J. L.; Wilson, L. J.; Curl, R. F.; Smalley, R. E.; *J. Phys. Chem.* **1990**, *94*, 8634.